Methodological study on single grain OSL dating of mortars: Comparison of five reference archaeological sites

Petra Urbanová, Pierre Guibert

DE GRUYTER OPEN

GEOCHRONOMETRIA 44 (2017): 77–97
DOI 10.1515/geochr-2015-0050

Available online at
http://www.degruyter.com/view/j/geochr

METHODOLOGICAL STUDY ON SINGLE GRAIN OSL DATING OF MORTARS: COMPARISON OF FIVE REFERENCE ARCHAEOLOGICAL SITES

PETRA URBANOVÁ[1] and PIERRE GUIBERT[1]

[1]IRAMAT-CRP2A, "Institut de Recherche sur les ArchéoMATériaux - Centre de Recherche en Physique Appliquée à l'Archéologie", UMR5060 CNRS-Université de Bordeaux-Montaigne, Maison de l'Archéologie, Esplanade des Antilles, 33607 Pessac cedex, France

Received 9 August 2016 Accepted 7 December 2016

Abstract: The paper focuses on single grain OSL dating of quartz extracted from known age archaeological mortars, potentially representing a new tool for dating the construction of historical buildings. Apart from SG-OSL measurements and annual dose rate determination, the samples are systematically studied by means of optical microscopy, EDX-SEM cartography and beta autoradiography in order to evaluate the possible microdosimetric heterogeneity of each sample, arising principally from local variations of potassium content. Besides the practical aspects concerning sampling, preparation and appropriate choice of measurement conditions, the paper aims at the differences in microstructure and in elementary composition between different mortars and attempts to evaluate the impact of these aspects on the dispersion of equivalent dose distributions. Finally, archaeological doses (paleodoses) are calculated by using central age model (CAM), minimum age model (MAM) and internal-external consistency criterion (IEU). The appropriateness of these models for the exploitation of the measured SG-OSL data as well as for a hypothesis on the estimation of the input parameter needed to run these models are discussed. Three categories of mortars were identified: samples without any exploitable SG-OSL signal, samples that could have been reliably dated and poorly bleached samples affected by microdosimetric variations whose dating still remains complicated. Finally, the hypothesis on distinguishing between reliable and questionable dating results is raised and the potentials of the method for dating mortars are pointed out.

Keywords: mortar, single grain, OSL dating, quartz, archaeology.

1. INTRODUCTION

Apart from wide application in geology and sediment dating, optically stimulated luminescence dating (OSL dating) can also be employed to date architectural structures via the dating of construction mortars. This specific application, based on the premise that quartz aggregate can be optically bleached during the mortar preparation, firstly appeared in literature in 2000 (Bøtter-Jensen *et al.*, 2000) and has been tackled by several authors (Zacharias *et al.*, 2002; Goedicke, 2003; Jain *et al.*, 2004; Gueli *et al.*, 2010; Goedicke, 2011; Panzeri, 2013; Stella *et al.*, 2013). Many of these authors stated a difficulty with partial bleaching for a majority of tested samples which makes it impossible to date this kind of material by a standard single aliquot technique, consisting in the analyses of tens or hundreds of grains together.

Thanks to relatively recent developments of single grain attachments that are becoming a more and more frequently used tool for OSL analyses in recent years, the problem of age over-estimation arising from partial

Corresponding author: P. Urbanová
e-mail: Petra.Urbanova@u-bordeaux-montaigne.fr

ISSN 1897-1695 (online), 1733-8387 (print)

bleaching can be overcome. Recently published studies on mortar dating (Urbanová *et al.*, 2015; Urbanová *et al.*, 2016) demonstrate that mortar aggregate can contain a sufficient number of well-bleached quartz grains and thus show a real potential for dating the mortar by single grain OSL (SG-OSL).

The aim of this paper is to make a methodological overview on the dating of mortars by SG-OSL after a three year experiment carried out in the Bordeaux laboratory of archaeometry IRAMAT-CRPAA. SG-OSL analyses of 35 mortar samples originating from five different monuments will be compared. The objective is to discuss all the aspects from the sample preparation via specificities of the measurement protocol and data evaluation to the age estimation, thereby underlining the importance of material characterization prior to the SG-OSL analysis. Finally, we will attempt to suggest a convenient analytical protocol for dating mortars by SG-OSL based on currently available analytical methods, and we will assess current advancements as well as persistent limitations.

2. STUDIED SAMPLES

The mortar samples presented in this paper come from the monuments that were all independently dated by other physical (archeomagnetism or radiocarbon dating) or archaeological and historical approaches. The aim of the study was to have diversified samples regarding age and geological origin, to look into differences between them and thence to draw more general conclusions concerning their dating potential.

The SG-OSL dating results presented in **Table 1** refer to the mortar samples originating from the following archaeological monuments:

- the Grimaldi castle in Antibes, French Riviera, France (Urbanová *et al.*, 2016; Guérin *et al.*, 2015)
- the *Palais-Gallien* amphitheatre in Bordeaux, *Aquitaine*, France (Hourcade *et al.*, 2011; Hourcade, 2013; Urbanová *et al.*, 2015)
- the Saint Seurin basilica in Bordeaux, *Aquitaine*, France (Michel, 2012; Urbanová and Guibert, 2017; a detailed publication on archaeological and archeometric study of mortars from this monument is being prepared)
- the Roman baths of Chassenon, *Charente-Maritimes*, France (Hourcade *et al.*, 2010; Hourcade and Mourin, 2013)
- Basel cathedral, Switzerland (Fischer, 2008)
- mortar mixers excavated on three different archaeological sites in Switzerland (Hueglin, 2011)

The results of SG-OSL dating of the last three above mentioned archaeological sites (Chassenon, Basel and Swiss mortar mixers) have not been published separately before and are not part of any publication in preparation.

3. METHODS AND MATERIALS

Sampling

The sampling of mortars was performed in the zones attributed with certainty to the original constructions of each monument, avoiding restored or reconstructed areas. Three different sampling procedures were employed, depending on the solidity of the mortar:

- extremely resistant, hard mortars were taken using a core drill of 50 mm in diameter designed for wet cutting (generally Gallo-Roman mortars or mortars from narrow joints where other ways of sampling are difficult to carry out)
- more fragile mortars were sampled by means of a chisel and a hammer
- highly brittle mortars were scraped off from an inner part of a wall after removing a surface layer, all the procedure being performed under dark light conditions (a dark area or an impervious canvas)

The use of a core drill often represents the only possible way of sampling if the mortar is solid and occurs in very thin layers in standing brick or stone masonry. However, such an intervention has to be performed under water cooling, which affects the original water content of the sample. Also, sampling by scraping off has a drawback, since thin and thick sections of the sample cannot be prepared and material characterization is limited to chemical analyses of powder. The sampling using a chisel and a hammer is therefore preferred, if possible, since it allows the obtaining of samples without biasing their initial on-site humidity and its parts can be used to prepare thin and thick sections for characterization of the material in question.

SG-OSL analyses

Preparation of samples for SG-OSL analysis and a quantity needed

The aim of the preparation procedure for single SG-OSL measurements in this experiment was to extract the quartz grains of the size fraction 200–250 µm that were not exposed to light during sampling, following the hypotheses that the coarser fraction is supposed to be better bleached in the case of mortar (i.e. Goedicke, 2003; Jain *et al.*, 2004). If the samples are compact, the external part that might have been briefly exposed to light during sampling is scraped off. In order to do so, the use of manual tools is preferable to using a saw since the latter causes quite important loss of material and there is a risk of sample disintegration during cutting. After removing a surface layer, the internal part of the sample is gently crushed into powder and sieved. If mortar has been sampled in dark light conditions in the form of powder, it can be directly sieved.

Table 1. *List of studied monuments with corresponding historical periods, reference date intervals, reference dating methods, mortar function in masonry and sample numbers. For more details about the list of mortar samples, the reader is referred to Urbanová et al. (2016) for Antibes, to Urbanová et al. (2015) for Palais-Gallien and to Urbanová and Guibert (2017) for Saint Seurin. For more details about reference dates, the reader is referred to Lanos and Dufresne (2013) for Antibes, to Hourcade (2013) and Lanos and Dufresne (2013) for Palais-Gallien, to Michel (2012) for Saint Seurin, to Hourcade and Maurin (2013) and Lanos and Dufresne (2013) for Chassenon, to Fischer (2008) for Basel and to Hueglin (2011) for mortar mixers.*

Site	Historical period	Reference date interval	Reference dating method	Mortar function	Sample number
Antibes	Gallo-Roman	[9 BC, 72 AD] TPQ*: [60 AD, 100 AD]	Archaeomagnetism (bricks) Archaeology	Mortar binding stones	BDX 16045 BDX 16046 BDX 16047 BDX 16048 BDX 16049
Chassenon	Gallo-Roman	[82 AD, 178 AD] [90 AD, 170 AD]	Archaeomagnetism (bricks) Archaeology	Boarding mortar Mortar binding stones Mortar binding stones	BDX 15628 BDX 15636 BDX 15638 BDX 15639
Palais-Gallien	Gallo-Roman	[68 AD, 150 AD] [90 AD, 170 AD]	Archaeomagnetism (bricks) Archaeology	Mortar binding bricks Mortar binding bricks Foundation mortar Foundation mortar	BDX 15541 BDX 15542 BDX 15543 BDX 15544
St Seurin	Late Antiquity & Early Middle Ages crypt	Posterior to BDX 16493 TPQ: 1100 AD	Archaeology	Filling mortar (floor)	BDX 16492
		Posterior to BDX 16496 TPQ: 1100 AD	Archaeology	Filling mortar (floor)	BDX 16493
		[305 AD, 562 AD] TPQ*: [658 AD, 783 AD]	TL and OSL (bricks) Radiocarbon (charcoal)	Ground mortar Ground mortar Ground mortar (floor)	BDX 16496 BDX 16498 BDX 16500
	Romanesque apse	[810 AD, 910 AD]	Historical sources	Mortar binding ashlars	BDX 16592 BDX 16593 BDX 16594
	Gothic chapel	[570 AD]	Historical sources	Mortar binding ashlars	BDX 16586 BDX 16587 BDX 16591
Basel	Gallo-Roman	[270 AD, 350 AD]	Historical sources	Ground mortar (*hypocaust*)	BDX 16304
	Late Antiquity & Early Middle Ages	[300 AD, 800 AD]	Archaeology	Mortar binding stones	BDX 16293 BDX 16299
	Carolingian	[790 AD, 890 AD]	Archaeology	Mortar binding stones	BDX 16301 BDX 16303
	Ottonian	[890 AD, 990 AD]	Archaeology	Mortar binding stones	BDX 16288 BDX 16294
	Romanesque	[1100 AD, 1200 AD]	Archaeology	Mortar binding stones	BDX 16295
Basel	Romanesque	[936 AD, 1018 AD]	Radiocarbon (charcoal)	Mortar from mortar mixer	BDX 16306
Müstair	Romanesque	958 AD	Historical sources	Mortar from mortar mixer	BDX 16308
Zurich	Romanesque	[853 AD, 874 AD]	Historical sources	Mortar from mortar mixer	BDX 16309

**terminus post quem*

The chemical treatment includes three stages: 10% HCl, 15% H_2O_2 and a mixture of H_2SiF_6 with HNO_3 in the ratio of 9 to 1 (Urbanová *et al.*, 2015). The last step takes about 1–2 weeks depending on the quantity of feldspars to be dissolved. A total dissolution of feldspar in the etched fractions from mortars is verified before starting the dating procedure by IRSL test (Urbanová *et al.*, 2015). The external alpha contribution to the annual dose ("k" value) taken into account in this work is equal to 0.05 ± 0.02 (Blain *et al.*, 2007; Guibert *et al.*, 2009a; further details in Urbanová *et al.*, 2015).

The quantity of the bulk sample needed for the preparation is variable, depending on the abundance and the grain size of quartz in mortar. Nevertheless, between 50–100 g of raw material was generally sufficient to obtain between 200 and 500 mg of quartz size fraction 200–250 μm.

The amount of quartz grains necessary for SG-OSL analyses including measurements of equivalent doses, dose recovery tests and IRSL tests depends on the proportion of luminescent grains in the sample and its degree of bleaching. To give a general idea, for the well-bleached sample with 5% of luminescent grains we needed about

53 mg of material (3800 quartz grains of size fraction 200–250 μm) to obtain the distribution of 190 individual equivalent doses.

OSL instrumentation

All OSL measurements were performed using a TL/OSL DA20 Risø reader. The light detection system of the reader consists of an EMI Q9235 photomultiplier tube and 7.5 mm of Hoya U-340 filter for detection in the UV-blue wavelength range (about 280–370 nm). A $^{90}Sr/^{90}Y$ beta source was used as an irradiation source (dose rate 0.150 ± 0.005 mGy/s on the 1st January 2014). Two different luminescence stimulation systems depending on the measurement protocol were used. The OSL measurements by a standard multigrain technique use Blue LEDs (NISHIA type NSPB-500s) with a peak emission at 470 nm for the stimulation, while a single grain analysis was performed by a 10 mV Nd: YVO_4 solid state diode-pumped laser emitting at 532 nm.

OSL measurements and data evaluation

The measurements of recovery dose and equivalent doses were performed applying the SAR protocol (Murray and Wintle, 2000) using the parameters described in **Table 2**. OSL signals from multi-grain aliquots are based on the summation of the first 0.8 s of stimulation corrected for background derived from the last 8 s (time of stimulation: 40 s). Single-grain OSL signals are derived from the summation of the first 0.05 s of stimulation less the sum of the last 0.2 s (time of stimulation: 1 s). For each grain or disc, the sensitivity-corrected regenerated OSL signals (L_x/T_x) were fitted with an exponential function and each individual equivalent dose (D_e) was estimated by projecting the sensitivity-corrected natural signal (L_N/T_N) onto the fitted curve. The standard error on the individual equivalent dose was obtained by Analyst version 4.11 from counting statistics, curve fitting and the instrumental reproducibility error of 2.7% (the value calculated from the series of measurements performed in the IRAMAT-CRPAA laboratory in Bordeaux).

In general, single grain analyses reveal significant heterogeneity of luminescent properties between individual grains. Such heterogeneity cannot be noticed by any classical multigrain technique because of averaging effects that occur when tens or hundreds of grains are measured together. Selection criteria used to evaluate single grain measurements should therefore be logically less strict than for multigrain analyses. In this work, the grains were retained following criteria mentioned below also used by other authors dealing with weakly luminescent samples (for example Thomsen *et al.*, 2004; Jacobs *et al.*, 2006, 2013; Medialdea *et al.*, 2014):

1) relative error on recycling ratio error did not exceed 25% (related to the reference value 1)
2) the error associated with the T_N signal was <25%
3) the signal was more than 3 sigma above background

The influence of the selection criteria on the global archaeological dose (paleodose) was evaluated by comparing the archaeological dose calculated for all the grains giving a signal with the archaeological dose obtained only when the selected grains were taken into account. Even if no significant differences were observed in our case, we still consider the application of these criteria justified for obtaining reliable estimates of equivalent doses.

Dose rate determination

Contributions of different dose rate components used for the age calculation were evaluated. The α and β contributions of the sample matrix were determined by low background gamma spectrometry (Guibert and Schvoerer, 1991, Guibert *et al.*, 2009b) that allows K, U and Th contents of dated material to be obtained and converted into the related dose rates using the conversion factors published by Guérin *et al.* (2011). Dose attenuation coefficients of α and β dose rates in coarse grains were calculated according to Mejdahl (1979) and Brennan *et al.* (1991). The environmental dose rate contribution was measured by Al_2O_3 dosimeters, left during a period of 8–15 months *in situ* (depending on each monument). The internal radioactivity of quartz grains used for dating was evaluated by inductively coupled plasma mass spectrometry (ICP-MS).The practical aspects and measurement protocols on all the above-mentioned analyses are described in detail in Urbanová *et al.* (2015).

For the majority of studied samples, water content could not be precisely measured because the sampling by the core drill biased their initial humidity. In addition, the humidity could have fluctuated in the past. An approximate contribution of water content to the annual dose rate

Table 2. *Measurement parameters used for the determination of individual equivalent doses.*

Site	Preheat (°C)	Cut-heat (°C)	Test dose (Gy)	Recovery dose (Gy)	Regeneration doses (Gy)
Grimaldi castle, Antibes	240	190	4.8	4.8	4.8, 9.6, 14.4, 19.2, 0, 4.8
Thermal baths of Chassenon	220	190	4.8	4.8	4.8, 9.6, 14.4, 19.2, 0, 4.8
Palais-Gallien, Bordeaux	240	190	4.8	4.8	4.8, 9.6, 14.4, 19.2, 0, 4.8
Basel cathedral, Basel	190	160	1.5	1.5	0.75, 1.5, 4.5, 10.5, 0, 0.75
Saint Seurin crypt, Bordeaux	190	160	3	3	1.5, 3, 6, 12, 0, 1.5
Saint Seurin apse/chapel, Bordeaux	190	160	1.5	1.5	0.75, 1.5, 4.5, 10.4, 0, 0.75
Mortar mixers (Basel, Müstair, Zurich)	190	160	3	3	1.5, 3, 6, 12, 0, 1.5

was estimated from the difference in weight between the dry sample and the same sample saturated with water, assuming 50% of the saturation value for elevated parts of masonry and 75% for samples from foundations. Relative error on estimated water content was taken equal to 50%. The values taken into account for the age calculation are presented in **Table 7**.

Material characterization

The mortar samples were studied by optical microscopy, beta autoradiography and scanning electron microscopy coupled with energy dispersed X-ray spectroscopy (SEM-EDX). The objective was to assess chemical composition, nature, form and size of the aggregate and the distribution of beta emissions in the matrix. The SEM-EDX analyses were carried out in a low vacuum mode (pressure: 25 Pa; LV: 20 kV) using the electron microscope JEOL 6460 LV coupled to an EDS spectrometer composed of an SDD semi-conductor (Oxford INCA 30 spectrometer). Any other details on instrumental equipment used and on measurement parameters employed can be found in Urbanová *et al.* (2015).

4. RESULTS AND DISCUSSION

Luminescent characteristics

As already observed by other authors, for mortars and young sediments (Jacobs *et al.*, 2013; Sim *et al.*, 2013; Medialdea *et al.*, 2014), only a low proportion of grains responds to the OSL stimulation. **Table 3** sums up the luminescent characteristics of mortars presented in this paper. While for the samples from Antibes, *Palais-Gallien* and Saint Seurin the proportion of selected luminescent grains is between 2.4 and 7.0%, the mortars from Chassenon and Basel show extremely low sensitivity. For 5 out of 8 of the Basel samples and all 3 mortar mixer samples, no exploitable signal (neither natural, nor regenerated) was detected.

The capacity of quartz grain to give the OSL signal seems to depend on the number of OSL traps and luminescent centers whose existence is related to the presence of defects and impurities in the quartz crystal lattice (e.g. Krbetschek *et al.*, 1998; Götze *et al.*, 2001). The sensitivity of quartz to OSL stimulation is therefore directly linked to its geological origin and to the conditions in which a crystal has been formed. Also, according to some authors (Ruffer and Preusser, 2009), luminescence intensity and a number of grains sensitive to OSL stimulation can be affected by the environmental conditions to which minerals were subjected during their existence, such as repetitive cycles of irradiation, bleaching and solar heating that cause, according to some authors, for example, the high sensitivity of "Australian" quartz (Pietsch *et al.*, 2008).

If we consider that the sand used to prepare the Basel mortars originates from the local geological environment, it may seem that quartz from this region is not favorable for use as a natural dosimeter due to its very low sensitivity. Nevertheless, larger number of studied samples with similar origins would be necessary to confirm this hypothesis. From this point of view, it would be interesting to carry out a study on the relationship between the geological provenance of mortar aggregate and its dating potential. We are trying to develop this aspect in future experiments which would be very helpful in predicting the dating potential of mortars in general.

Sense and validity of preliminary tests for SG-OSL analyses

Specificities of SAR protocol for mortars

The use of a SAR protocol for SG-OSL measurements on young samples with low sensitivity, such as mortars, needs to follow certain adjustments, unlike a standard procedure (Murray and Roberts, 1998). First, a test dose cannot represent 10% of an expected archaeological dose as is usually employed for sediments, since such low doses (about 0.1–0.3 Gy) would result in the loss of any OSL signal and in the impossibility of signal normalization. Therefore, a test dose between 1.5 and 4.8 Gy was employed. In addition, due to a supposed high variability of equivalent doses related to poor bleaching, a growth curve has to be sufficiently extended to estimate equivalent doses in a larger interval of values. The first two regeneration doses were chosen sufficiently close to the expected archaeological dose but still high enough to get the OSL response, while two higher regeneration doses were chosen 10 to 30 times higher to get an approximate equivalent dose estimation for poorly bleached grains. Nevertheless, the highest equivalent doses corresponding to extremely poorly bleached grains did not enter into this interval (see **Table 3**, the last column). The equivalent dose estimation of these grains is performed by the extrapolation of the exponential growth curve. If the proportion of such grains is significant, higher regeneration doses should be employed in order to extend the dose-response curve and to avoid the imprecisions in equivalent dose determination of the poorly bleached grains.

Preheat temperature, "plateau" test, thermal transfer and dose recovery tests

The choice of the convenient preheat temperature is crucial for a correct equivalent dose estimation. The preheat temperature should not be lower than 160°C in order to avoid unstable light sensitive traps contributing to a detected signal. However, a highly elevated temperature can provoke thermal transfer which can also negatively affect a measured luminescence.

The experiment on mortar dating was started with Gallo-Roman samples, being older and therefore generally more luminescent than mortars from younger periods.

Table 3. *Number of studied grains and proportions of luminescent and selected grains for all studied samples.*

Sample	Analysed grains		Luminescent grains		Selected grains		Grains above L_4/T_4*
	Nb	%	Nb	%	Nb	%	Nb
Grimaldi castle, Antibes							
BDX 16045	4085	100	200	5.0	196	4.8	0
BDX 16046	3800	100	193	5.0	180	4.6	1
BDX 16047	3800	100	179	4.8	175	4.7	5
BDX 16048	3990	100	205	4.9	189	4.5	0
BDX 16049	4085	100	163	3.9	152	3.6	1
Thermal baths of Chassenon							
BDX 15628	little quartz fraction 200-250 µm, no OSL signal						
BDX 15636	3895	100	67	1.7	61	1.6	9
BDX 15638	little quartz fraction 200-250 µm, no OSL signal						
BDX 16539							
Palais-Gallien, Bordeaux							
BDX 15541	2850	100	202	7.1	129	4.5	44
BDX 15542	1900	100	119	6.3	76	4.0	40
BDX 15543	4135	100	207	5.0	111	2.7	51
BDX 15544	4085	100	324	7.9	192	4.7	104
Saint Seurin crypt, Bordeaux							
BDX 16492	3800	100	275	7.3	176	4.6	57
BDX 16493	3800	100	233	6.1	145	3.8	52
BDX 16496	1995	100	99	5.0	32	1.6	26
BDX 16498	3800	100	152	3.8	71	1.9	49
BDX 16500	3800	100	127	3.1	90	1.9	21
Saint Seurin, apse, Bordeaux							
BDX 16592	3610	100	368	10.2	164	4.5	117
BDX 16593	3040	100	256	8.4	116	3.8	79
BDX 16594	3135	100	347	11.1	152	4.8	101
Saint Seurin, chapel, Bordeaux							
BDX 16586	2280	100	116	5.0	50	2.2	33
BDX 16587	3325	100	175	5.4	49	1.5	32
BDX 16591	-	-	-	-	-	-	
Basel cathedral (crypt)							
BDX 16304	3800	100	116	3.1	106	2.8	6
BDX 16293	analyzed by multigrain, very little OSL signal						
BDX 16299							
BDX 16301	2000						
BDX 16303	2000						
BDX 16288	2000		no OSL signal				
BDX 16294	2000						
BDX 16295	2000						
Mortar mixers							
BDX 16306	2000						
BDX 16308	2000		no OSL signal				
BDX 16309	2000						

** grains with the sensitivity-corrected natural signal (L_N/T_N) above the highest regenerated dose (L_4/T_4). The equivalent dose estimation of these grains is performed by the extrapolation of the exponential growth curve.*

The choice of measurement parameters was based on multigrain measurements which indicated the best results for the preheat temperatures about 240°C. Apart from single grain dose recovery measurements, preheat plateau tests and thermal transfer tests were performed by standard multigrain technique in order to verify the pertinence of this choice (e.g. Murray and Olley, 2002, Wintle and Murray, 2006; Medialdea *et al.*, 2014). However, exploitable results could have been obtained only for well bleached samples from Antibes (Urbanová *et al.*, 2016). Given that these tests are carried out by multigrain technique that allows the measurement of an average signal, it cannot be applied on poorly bleached samples with large scatter of equivalent doses. Performing the same tests by single grain technique would be a time-consuming procedure due to the generally low sensitivity of mortars to the OSL stimulation. Thus, for poorly bleached samples, the solution how to test the dependence of a natural dose on

preheat temperatures could be to perform two series of single grain measurements at two different preheat temperatures. This was done in the case of the sample BDX 15541 from *Palais-Gallien* for which no significant difference between the measurements at 190°C and 240°C was observed.

The single grain measurements of mortar samples from medieval monuments studied in the second part of the project were systematically carried out at 190°C. If the dose recovery ratio entered the interval 1.00 ± 0.10, the preheat temperature of 190°C was used for equivalent dose determination. Even if we did not observe any increase in equivalent dose with rising preheat temperature, we recommend using the preheat of 190°C and the cutheat of 160°C as initial parameters in order to minimize the potential risks of thermal transfer that would significantly change kinetics of luminescence. If the dose recovery tests are satisfactory, these temperatures can be kept for equivalent dose determination. The preheat temperature between 180–200°C for young samples is also recommended by other authors (Murray and Olley, 2002; Jain *et al.*, 2004; Goedicke, 2011; Medialdea *et al.*, 2014). The SG-OSL measurement parameters applied on the sample sets studied are detailed in **Table 2**.

Fast component and LM-OSL test

The OSL signal was dominated by the fast component for the quartz samples presented in this study, which is a primary condition for dating mortar. This aspect is usually evaluated by the LM-OSL test consisting in the linear increase of stimulation power during the OSL measurement. However, generally, this test can only be performed by multigrain technique as was the case in this study since routine experimental apparatus does not allow the performance of this kind of measurement by single grain procedure.

The presence of medium and slow components in the OSL signal can also be deduced from the form of the OSL decay curve. In this study, we systematically observed a very fast OSL decay during the first 0.1 s of stimulation for grains that showed they were well-bleached (**Fig. 1a**). On the contrary, for certain poorly bleached grains giving high equivalent doses the OSL decay was slower (**Fig. 1b**). The occurrence of medium

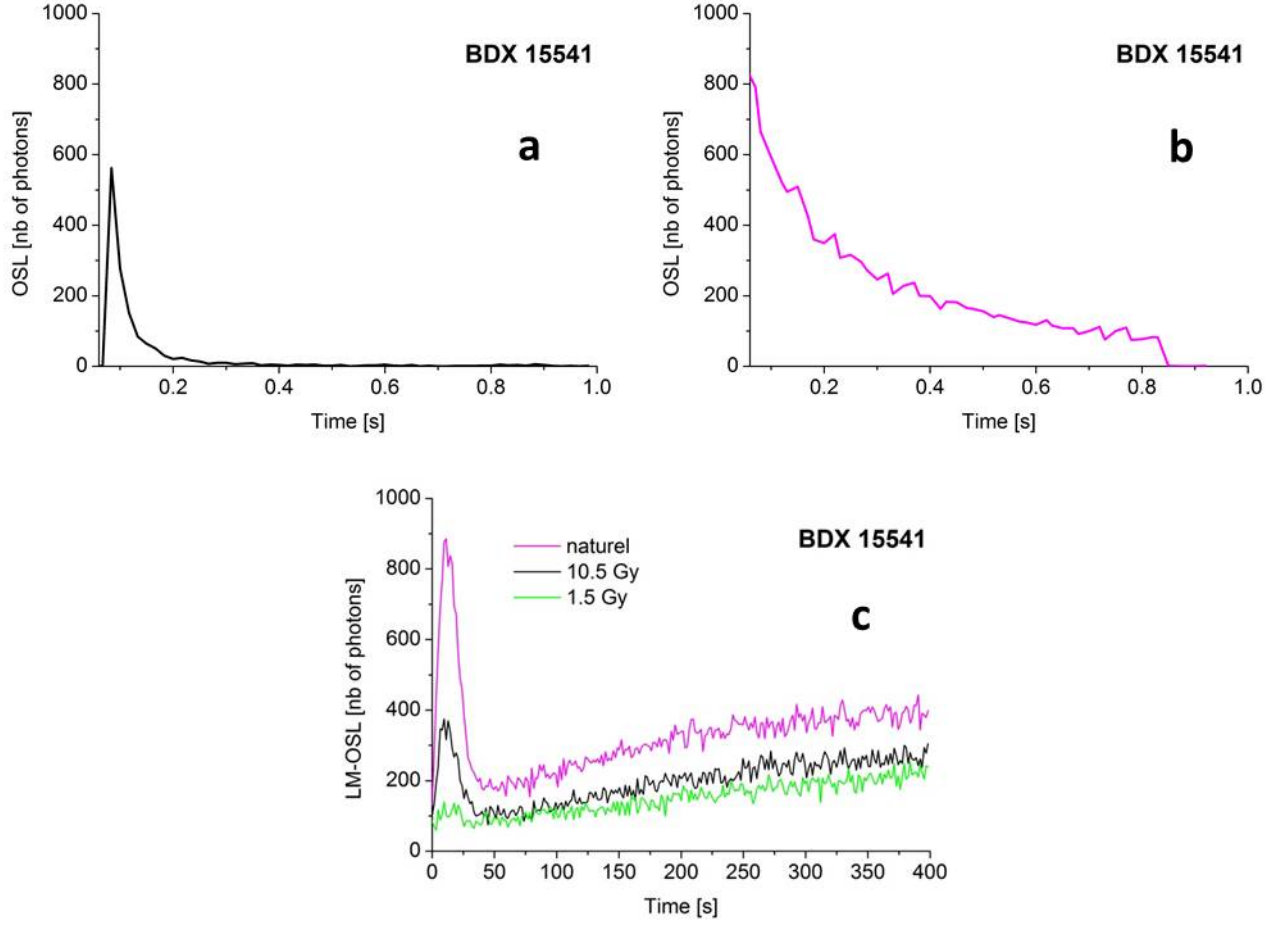

Fig. 1. *SG-OSL decay curve of well bleached (a) and poorly bleached (b) grain. (c) LM-OSL test of the sample BDX 15541 performed by the multigrain technique corresponding to an average signal of the mixture of poorly bleached and well bleached grains.*

and slow components in some cases of LM-OSL tests, as seen for some samples from Palais-Gallien and Saint Seurin (**Fig. 1c**), is principally linked to the presence of one or several poorly bleached grains with high signals on the same multigrain disc, but this does not characterize a behavior of all the grains on the disc (as observed also by Bulur *et al.*, 2001). Therefore, a classical LM-OSL test carried out on multigrain discs gives only an average signal and is not a reliable and direct indicator of luminescent properties for individual grains.

Distributions of equivalent doses and their representation

Fig. 2 shows some selected distributions of equivalent doses for mortar samples originating from different monuments, some of them having already appeared in corresponding publications. Visually, the histograms in **Figs. 2a**, **2b** and **2c** corresponding to Antibes, Chassenon and Gallo-Roman Basel mortar show narrow distributions centered around the value of 3, 11 and 2 Gy, respectively. The distributions in **Figs. 2d**, **2e** and **2f** show a scattering of values with the high frequency peak around 2–4 Gy corresponding to the expected archaeological doses and with a long tail going up to 100 Gy or more.

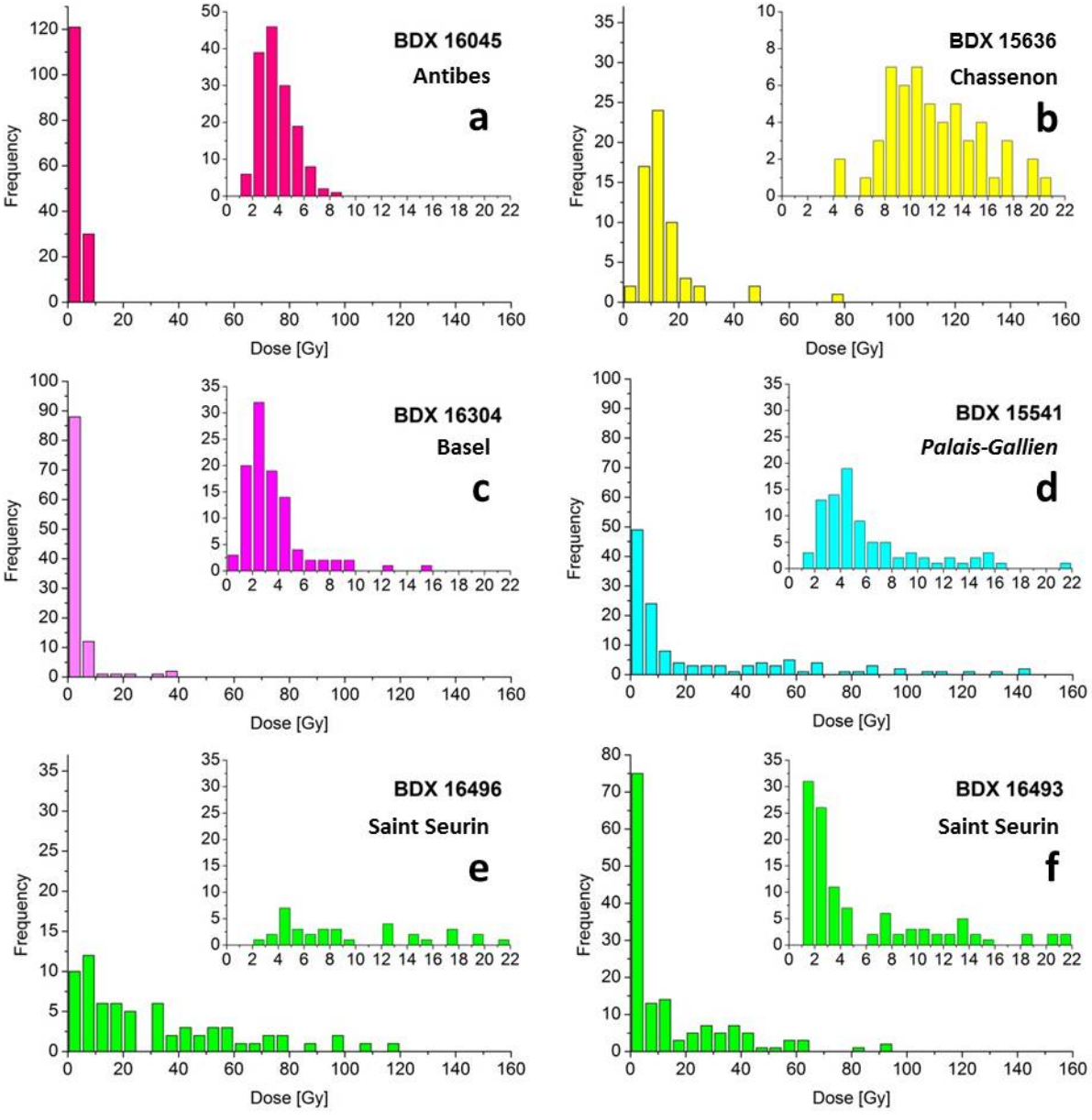

Fig. 2. *Histograms (a-f) show the distributions of individual equivalent doses from SG-OSL measurements.*

A representation by histograms was chosen for the fast visual evaluation of the spread of equivalent doses. The bin size is equal to the median value of absolute standard errors. However, we are aware of the weak point of representation by histogram which consists in a lack of information on standard error distribution. Corresponding distributions of relative errors are shown in **Fig. 3**. The influence of the elimination of equivalent doses with high relative errors on the form of the histogram was evaluated, and the conclusion is that this difference was not visually recognizable.

Sources of dispersion in equivalent dose distributions

The sources of dispersion in single grain equivalent dose distributions of mortars have already been identified and discussed in previous studies (Urbanová *et al.*, 2015, 2016) and appear in other publications on single grain dating of sediments (Thomsen *et al.*, 2005). We recall here the concept of the four principal factors contributing to the scatter in equivalent dose distributions:

- measurement uncertainty noted s_i for the grain i (including errors on counting statistics, instrument reproducibility, heterogeneity of the source and curve-fitting)

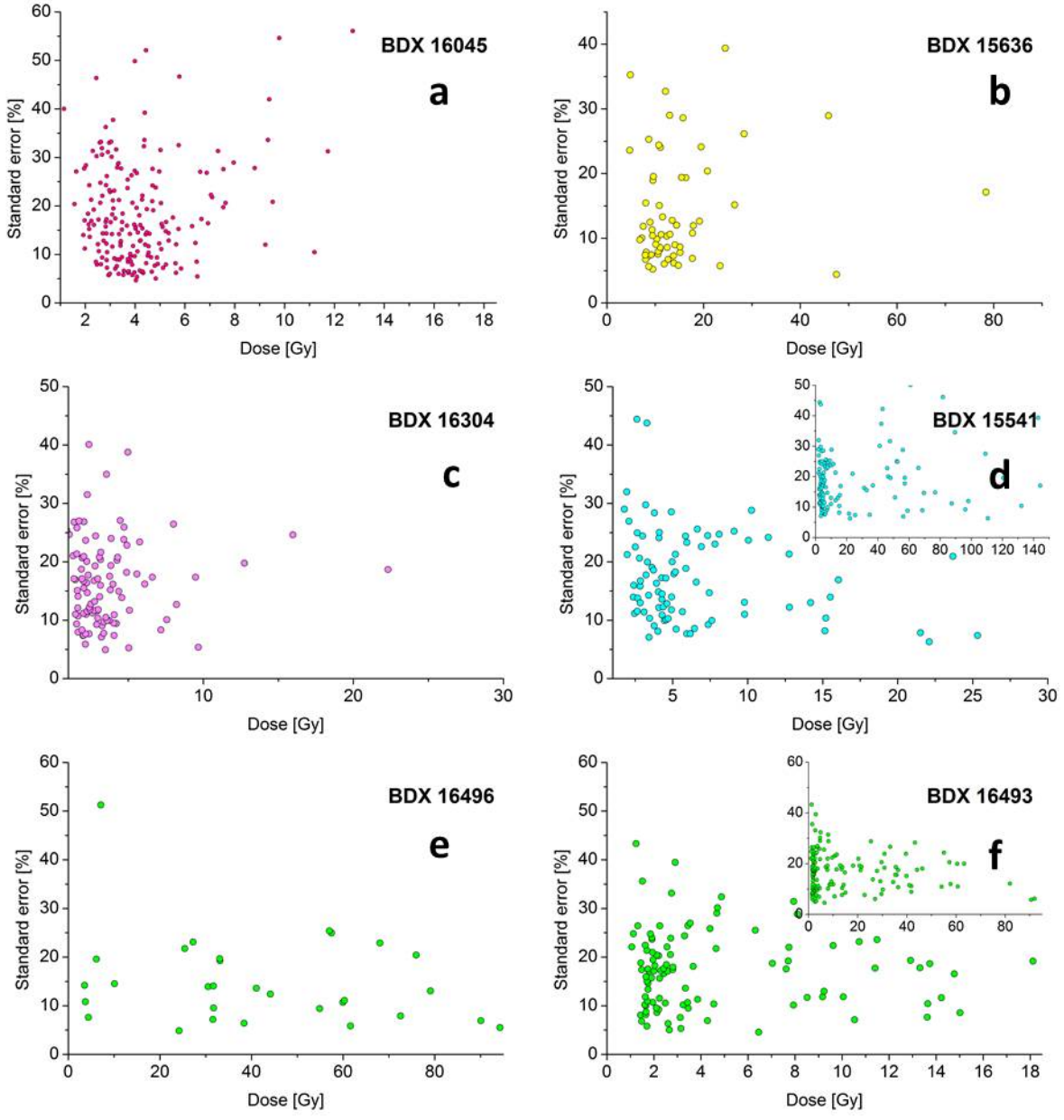

Fig. 3. *Distributions of relative errors related to ED distributions presented in the Fig. 2.*

- intrinsic variability σ_a ("additional uncertainty" following the terminology of Thomsen *et al.*, 2005 and 2007)
- variability of dose rates at the grain scale σ_m (microdosimetric variations)
- variability related to heterogeneous bleaching σ_x

The term "over-dispersion", which is, by definition, a quantification of unexplained variance in the data (Thomsen, 2012), covers the last three of them. Based on the largely used Central age model (CAM, Galbraith *et al.*, 1999), over-dispersion is expressed as a relative uncertainty added in quadrature to the statistical variance of each individual value of measured equivalent dose, assuming additivity of variances: $\sigma^2 = \sigma_a^2 + \sigma_m^2 + \sigma_x^2$. We would like to underline that these factors cannot be considered as a real "uncertainty" since all of them are natural characteristics of the studied material. The impossibility of distinguishing between individual contributions of each factor represents the principal difficulty in evaluating scattered single grains distributions. In the following paragraphs, the way of evaluating each of these factors is attempted and their possible impact on the dating procedure is assessed.

Intrinsic variability

"It is clear that there is significant over-dispersion in natural well-bleached samples, but some studies have also shown that there is significant over-dispersion even in laboratory dose recovery experiments where all extrinsic sources of variability have been eliminated." (Thomsen *et al.*, 2012) That is what we call "intrinsic variability". **Table 4** presents over-dispersion values from dose recovery measurements (OD DRT) of mortar samples bleached artificially in the laboratory. In this first case, over-dispersion corresponds to intrinsic variability. At the same time, over-dispersion values from equivalent dose measurements (OD ED) of natural mortar samples are shown. In this second case, only part of over-dispersion is accounted for by intrinsic variability, while another part is caused by the combination of extrinsic factors. For all the samples, natural over-dispersion is systematically higher than over-dispersion from dose recovery tests.

If we assume a transmissibility of properties in grains analyzed in DRT tests to grains used for ED measurements, the difference between OD ED values and OD DRT values will give an approximate contribution of poor bleaching and microdosimetric effects to the scatter in ED distributions. One must be conscious of the fact that DRT tests are not performed on the same set of grains as the ED measurements and that the process of artificial bleaching only simulates the process of natural bleaching, so some differences can occur. In our experiment, dose recovery ratio values on the samples artificially bleached in a solar simulator were about 0.05–0.09 more elevated than when the same samples were bleached directly in the OSL reader (Murray and Wintle, 2000). Similar discrepancies were also observed by Choi (Choi *et al.*, 2009), who raised the hypothesis that the ultraviolet component of the solar simulator source may provoke excitation of deep OSL traps, contributing consequently to the measured OSL signal. Other experiments focused on the comparison of different kinds of artificial bleaching would be useful in future.

Table 4. *Over-dispersion values (OD) obtained by using Central age model (Galbraith et al., 1999) from dose recovery experiments (DRT) and equivalent dose measurements (ED) and estimation of extrinsic variability calculated as the difference between OD ED and OD DRT.*

Sample	OD DRT (%)	OD ED (%)	Extrinsic variability (%)
Grimaldi castle, Antibes			
BDX 16045	14 ± 2	31 ± 2	28 ± 4
BDX 16046	12 ± 2	31 ± 2	29 ± 4
BDX 16047	8 ± 2	43 ± 3	42 ± 4
BDX 16048	7 ± 2	27 ± 2	26 ± 4
BDX 16049	5 ± 2	36 ± 2	36 ± 4
Thermal baths of Chassenon			
BDX 15636	5 ± 2	45 ± 5	45 ± 7
Palais-Gallien, Bordeaux			
BDX 15541	13 ± 2	121 ± 8	120 ± 10
BDX 15542	5 ± 2	129 ± 8	129 ± 10
BDX 15543	16 ± 3	148 ± 10	147 ± 13
BDX 15544	8 ± 2	144 ± 8	144 ± 10
Saint Seurin crypt, Bordeaux			
BDX 16492	14 ± 2	129 ± 7	128 ± 9
BDX 16493	8 ± 2	128 ± 8	128 ± 10
BDX 16496	12 ± 3	96 ± 13	95 ± 16
BDX 16498	15 ± 4	106 ± 9	105 ± 13
BDX 16500	16 ± 3	117 ± 9	116 ± 12
Saint Seurin, apse, Bordeaux			
BDX 16592	10 ± 3	136 ± 8	136 ± 11
BDX 16593	-	148 ± 10	-
BDX 16594	-	134 ± 8	-
Saint Seurin, chapel, Bordeaux			
BDX 16586	7 ± 4	157 ± 16	157 ± 20
BDX 16587	-	148 ± 15	-
Basel cathedral (crypt)			
BDX 16304	9 ± 2	68 ± 5	57 ± 14

Since OD DRT represents the best estimation of intrinsic variability when no well-bleached variant of poorly bleached sample to be dated is available (Thomsen *et al.*, 2012), we suggest performing artificial bleaching in the OSL reader, that generally gives satisfactory results. As we will see further, these measurements will be important for the use of minimum age models.

Microdosimetric variations in mortar samples and implications for dating

Microdosimetric variations can be caused by the heterogeneous distribution of radioelements in the mortar matrix. As a consequence, despite the fact that two grains could have been well-bleached when the building was constructed, they will give two different equivalent doses. Taking into account the size of the mortar samples from

which quartz grains for dating purposes are extracted, we assume that these grains received the same gamma and cosmic annual dose rates. By contrast, we consider that if some microdosimetric variations at the grain scale occur, these are principally due to the heterogeneity of beta irradiations, originating from three series of radioelements: potassium-40, the series of thorium-232 and the series of uranium-238 and uranium-235. Among minerals contained in mortar, potassium is mainly present in potassium feldspars, in micas and in certain clays, whereas uranium and thorium can be found in abundance in heavy minerals such as zircons or apatites. Three analytical methods were used to assess microdosimetric variations: petrography, beta autoradiography (**Fig. 4**) and cartography performed by scanning electron microscopy coupled with energy dispersed X-ray spectroscopy (SEM-EDX).

Beta autoradiography enables the study of the distribution of beta emissions in the mortar matrix, however, it does not make it possible to distinguish between different emitting radioelements (Ruffer and Preusser, 2009). Apart from the sporadic presence of zircons in the Antibes and Chassenon mortars, no significant quantity of zircons or apatites was noted in the rest of the studied samples. It was therefore assumed that the most important part of microdosimetric variations arises from potassium feldspars. SEM-EDX images in **Fig. 5** show elemental mapping of potassium in thick sections of different mortar samples studied. The higher the number of X rays emitted by potassium and detected by the instrument, the brighter the tones of grey obtained in corresponding spots that clearly correspond to potassium feldspars. The relationship between their quantity and size and microdosimetric variations expected is discused in the following paragraphs.

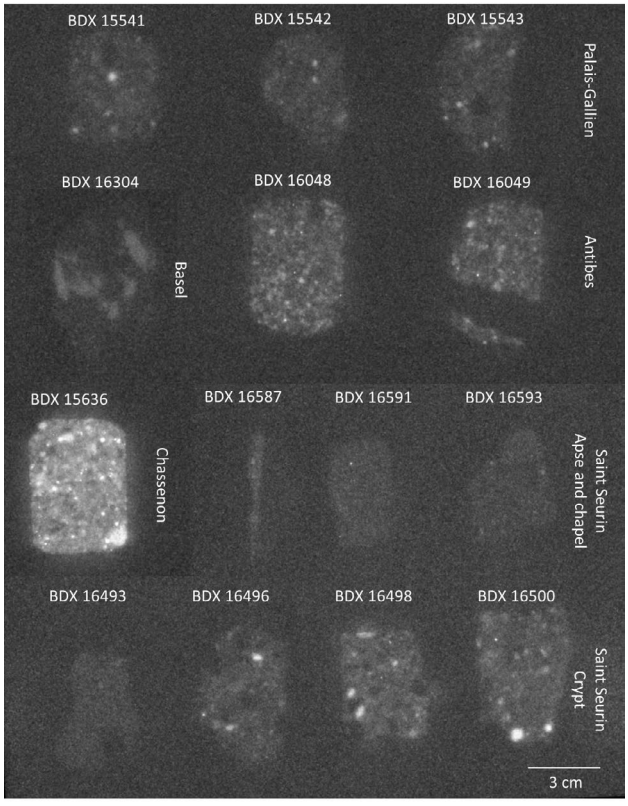

Fig. 4. *Beta-autoradiography images of different mortar samples. The brightest spots correspond to the most intense beta emitters.*

Small-grained mortars with low potassium content

The early medieval (BDX 16492 and BDX 16493), Romanesque (BDX 16593) and Renaissance samples (BDX 16587 and BDX 16591) from the Saint Seurin basilica in Bordeaux correspond to the group of the weakest radioactivity from mortars studied (**Fig. 4**). Hardly observable differences of tonality imply small relative variations in beta irradiations. Nevertheless, we have to mention that here we approach the detection limits of the method and the absence of differences in tonality does not necessarily mean that no variations occur.

According to SEM-EDX cartography and petrographic observations, all these mortars contain very low quantity of K feldspars. If some K feldspars occur (e.g. in the sample BDX 16493, **Fig. 5f**), their dimensions do not exceed 500 μm in diameter. A minor quantity of K feldspars partially explains low radioactivity and the apparent homogeneity of beta irradiations. Therefore, we assume that the contribution of microdosimetric effects to the dispersion in ED distributions won't be significant for this group of samples.

Small-grained mortars rich in potassium feldspars

Antibes (BDX 16045-9) and Chassenon (BDX 15636) mortars show higher radioactivity in comparison with the first group (**Fig. 4**). A high number of small bright points in beta images indicates that the majority of quartz grains is localized in close proximity to beta emitting minerals. Thus, beta irradiation effects will be more intense than in the first group, but they seem to be relatively homogeneous in the entire sample matrix. SEM-EDX cartography and a petrographic study show an abundance of K feldspars and zircons that are uniformly distributed in the mortar matrix (**Fig. 5a–b**), which is in agreement with the observations obtained by beta autoradiography.

Coarse-grained mortars with low potassium content

For Palais-Gallien mortars (BDX 15541-4), Roman Basel mortar (BDX 16304) and Saint Seurin *cocciopesto* mortars from the Late Antiquity period (BDX 16496, BDX 16498 and BDX 16500), the tonality of beta images is, in general, darker than in the case of the second group (**Fig. 4**). However, in certain areas, very bright spots corresponding to beta emitting minerals are observed. Due to their sporadic presence in the matrix, it is assumed that the effect of beta irradiation will be more spatially

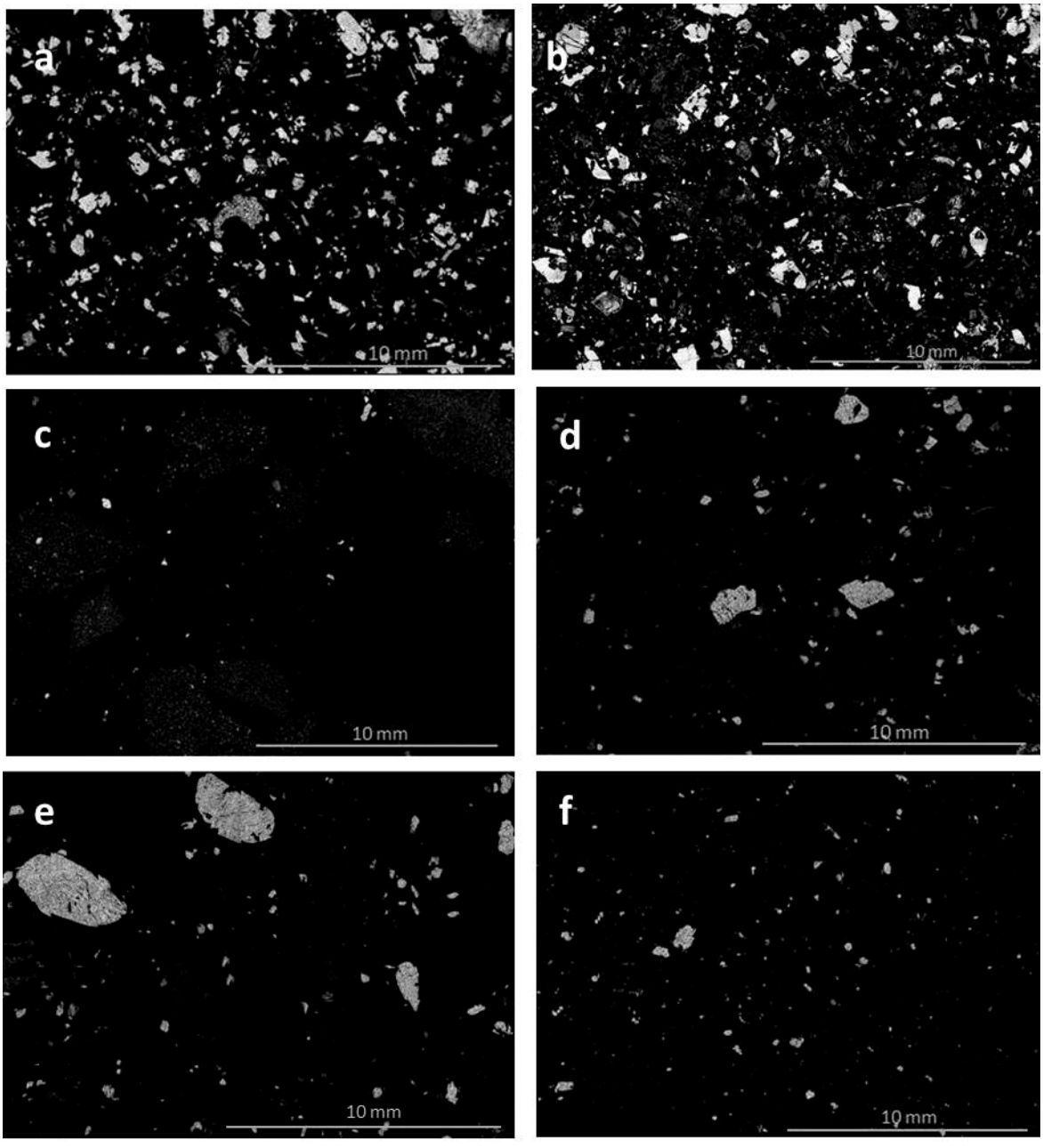

Fig. 5. *SEM-EDX carthography of potassium rich minerals in different mortar samples: (a) BDX 16048, (b) BDX 15636, (c) BDX 16304, (d) BDX 15541, (e) BDX 16496, (f) BDX 16493. The grey level corresponds to the number of X rays emitted by potassium detected by the instrument. Magnification: 60, pixel size: 0.03 mm.*

localized in this case, which implies highly heterogeneous microdosimetry for these mortar samples.

The mortars have a coarse-grained character visible even with the naked eye. SEM-EDX analyses showed the presence of K feldspars whose dimensions can reach several millimeters or even centimeters in diameter (**Fig. 5d–e**). In contrast, certain zones of mortar matrix contained exclusively large quartz. All these observations suggest that microdosimetric variations will probably significantly affect the scatter in ED distributions of these mortars.

It is worth mentioning a specificity of the sample BDX 16304. The mortar contains large *cocciopesto* (crushed brick) fragments of higher radioactivity in contrast with the rest of mortar matrix and this is demonstrated by globally brighter zones on the corresponding beta image (**Fig. 4**). The *cocciopesto* fragments are rich in potassium (**Fig. 5c**).

Local analyses of potassium (K) content

Apart from spatial visualization by SEM-EDX cartography, the potassium (K) content was assessed by local analysis including a radius of 2 mm (the radius corresponding to a penetration power of β particles) around the quartz grains used for OSL single grain measurements. It allowed the obtaining of distributions of K content in different zones of mortar matrix. The results are presented in **Table 5**.

Given that K content determined by EDX spectrometer does not contain the CO_2 correction and that low background gamma spectrometry is more sensitive than EDX in terms of detection limits, the K content measured by gamma spectrometry is considered to be more accurate. If we compare average values of K content determined by EDX and gamma spectrometry in **Fig. 6a**, we can see that the values obtained vary in the same way; a systematic standard deviation of these measurements is constant. Thus, we assume that K content measured by EDX spectrometer represents a reliable indicator of differences of K content in the studied mortars (see also Liritzis *et al.*, 2011).

We calculated an arithmetic mean of potassium content $\boldsymbol{K}$ determined by SEM-EDX in different zones of each mortar sample and its standard deviation $\boldsymbol{\sigma}$ for the number of measurements $\boldsymbol{n}$. In **Fig. 6b** we can see the increasing tendency of $\boldsymbol{\sigma}$ as the function of $\boldsymbol{K}$. We also calculated a relative variability of K content $\boldsymbol{\sigma_{relative}}$ as the ratio between $\boldsymbol{\sigma}$ and $\boldsymbol{K}$. $\boldsymbol{\sigma_{relative}}$ decreases for higher $\boldsymbol{K}$ which indicates that relative variability of potassium content is more significant for mortars with lower potassium content (**Fig. 6c**; for example *Palais-Gallien* mortars BDX 15541-3). In contrast, for mortars rich in potassium with high values of $\boldsymbol{K}$, such as the Chassenon or Antibes samples, relative variations of potassium content $\boldsymbol{\sigma_{relative}}$ are lower.

It is necessary to underline another important factor. The K content of BDX 16587 from the Saint Seurin crypt and the Palais-Gallien mortars is very similar, however, the relative variability $\boldsymbol{\sigma_{relative}}$ is much lower for BDX 16587. This can be explained by the presence of small K feldspars (maximum 500 μm in diameter) in the first case in contrast to K feldspars of a millimetric or centimetric scale in the second one. The distribution of potassium in the matrix of BDX 16587 is therefore more uniform. The observations correspond to above mentioned results that the combination of lower potassium content with coarse-grained material will provoke more significant microdosimetric variations. Our conclusions are also in agreement with the statements of Guérin *et al.* (2015) and Mayya *et al.* (2006).

Table 5. *Results of the local analyses of potassium (K) content in thick sections of studied mortar samples, obtained by SEM-EDX. We introduce: n — number of analysis; K_{min} — the lowest measured value of K content; K_{max} — the highest measured value of K content; K_{mean} — arithmetic mean of K content for n measurements; σ_K — standard deviation of arithmetic mean K_{mean} for n measurements; σ_{rel} — relative standard deviation calculated as the ratio of σ_K to K_{mean}; K_{gamma} — K content determined by low background gamma spectrometry.*

Sample	*n*	K_{min} (%)	K_{max} (%)	K_{mean} (%)	σ (%)	σ_{rel}	K_{gamma} (%)	*CaO* (%)
Antibes								
BDX 16045	31	0.33	3.64	0.98	0.64	0.65	1.43	30
BDX 16046	-	-	-	-	-	-	1.44	-
BDX 16047	-	-	-	-	-	-	1.88	-
BDX 16048	22	1.13	2.86	1.69	0.44	0.26	1.94	-
BDX 16049	35	0.84	2.30	1.44	0.32	0.22	1.74	26
Chassenon								
BDX 15636	17	1.48	3.56	2.71	0.55	0.20	2.86	33
Palais-Gallien								
BDX 15541	29	0.12	1.10	0.53	0.27	0.50	0.85	26
BDX 15542	40	1.17	2.26	0.85	0.51	0.60	1.13	-
BDX 15543	33	0.04	1.09	0.43	0.27	0.62	0.80	29
BDX 15544	-	-	-	-	-	-	0.67	25
St Seurin								
BDX 16492	13	0.11	1.11	0.59	0.41	0.58	0.43	22
BDX 16493	51	0.03	1.11	0.30	0.23	0.78	0.47	26
BDX 16496	24	0.12	2.24	0.80	0.46	0.57	0.90	27
BDX 16498	56	0.07	2.58	0.83	0.66	0.80	0.87	23
BDX 16500	39	0.09	1.54	0.47	0.33	0.70	0.49	24
BDX 16592	-	-	-	-	-	-	0.60	54
BDX 16593	15	0.12	0.46	0.32	0.11	0.33	0.30	62
BDX 16594	-	-	-	-	-	-	0.30	56
BDX 16586	-	-	-	-	-	-	1.05	69
BDX 16587	9	0.68	1.93	1.17	0.38	0.33	1.03	62
Basel								
BDX 16304	38	0.27	1.39	0.68	0.31	0.45	0.44	61
BDX 16293	-	-	-	-	-	-	0.44	79
BDX 16299	-	-	-	-	-	-	0.55	63

Evaluation of bleaching degree

The last aspect to be evaluated is a bleaching degree. We considered that the mortar samples were well-bleached if the age calculation using the archaeological dose obtained with the Central age model (CAM, Galbraith *et al.*, 1999) was in agreement with the reference age, taking into account that all grains meet the selection criteria. Afterwards, we checked what could be an indication of good bleaching if the age of the sample wasn't known.

It was observed that for well-bleached mortars studied in this work over-dispersion values did not exceed 50%, whereas for poorly bleached mortars this value was systematically higher than 100%. These findings are in agreement with those suggested by Arnold *et al.* (2009). Also, well bleached distributions were symmetrical; the ratio of the lowest measured dose to the mean of the distribution (R_{min}, **Table 6**) was similar to the ratio of the mean of the distribution to the highest measured dose (R_{max}, **Table 6**). In contrast, for poorly bleached samples R_{max} was 2–3 orders of magnitude higher than R_{min} (**Table 6**). It is necessary to specify that the mentioned

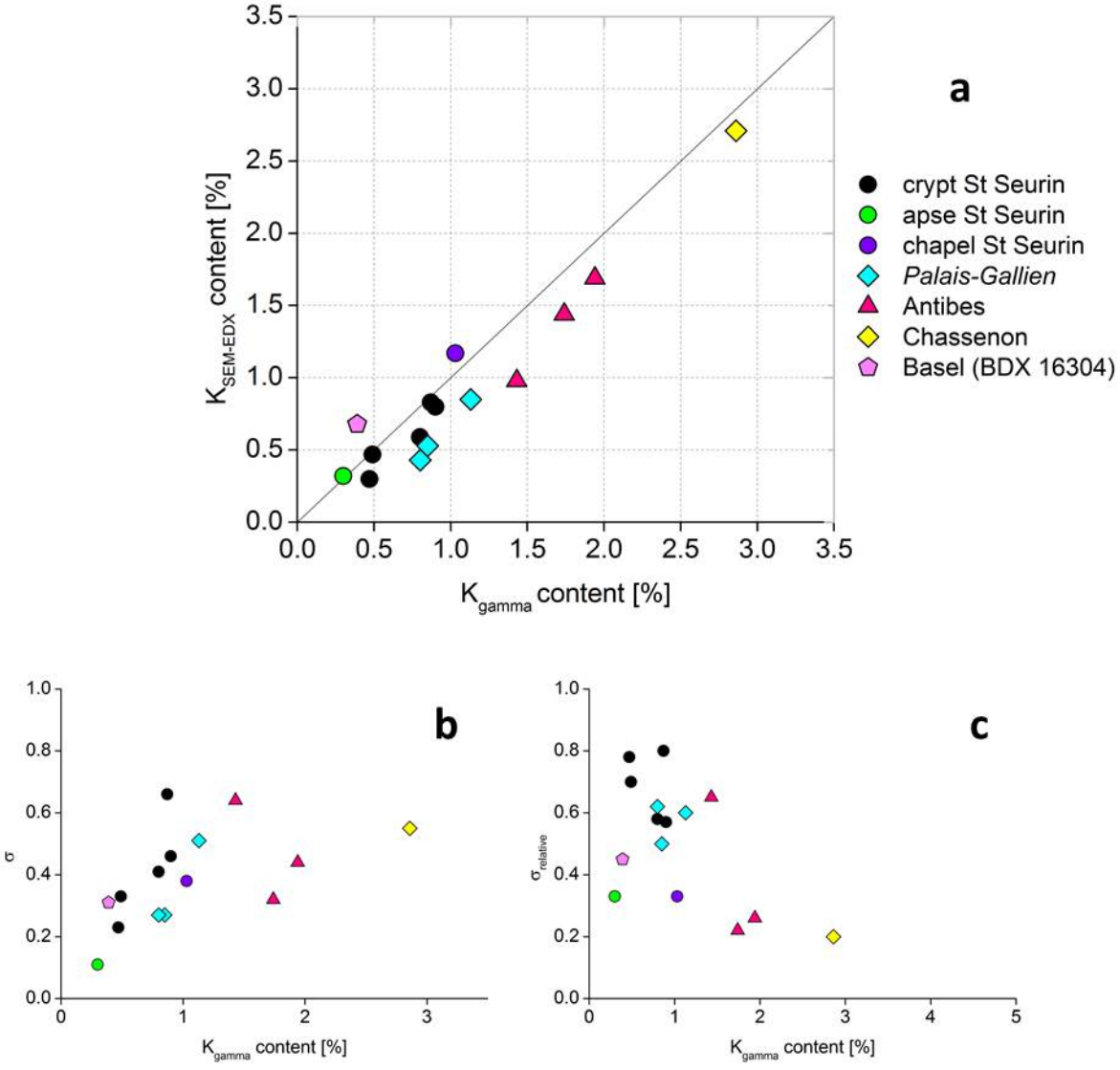

Fig. 6. *(a) Relation between the mean K content determined by low bacground gamma spectrometry and SEM-EDX analyses. (b) Standard deviation of the mean K content σ as the function of the mean K content determined by low background gamma spectrometry. (c) Relative variability of K content $\sigma_{relative}$ calculated as the ratio of standard deviation σ to the mean K content. Relative variability of K content is more significant for mortars with lower K content.*

criteria seem to be valid for all the studied mortars whose age does not exceed 2000 years. For Paleolithic sediments the asymmetry of the distribution can be less evident.

Calculation of archeological dose (paleodose) and age

Given that the mortar samples are not older than 2000 years, we prefer to use the term "archeological dose" instead of paleodose in the following paragraphs.

Well-bleached mortars (Antibes, Chassenon)

The samples identified as well bleached originate from Antibes, Chassenon and Basel as demonstrated by narrow ED distributions centered around the value of 3, 11 and 2 Gy, respectively (**Fig. 2**). All of them come from Antiquity or the late Antiquity period. Archaeological doses of these samples were determined by the Central age model (CAM, Galbraith *et al.*, 1999) and are presented in **Table 7**.

For the Antibes and Chassenon mortars, we observe agreement between the reference ages and the ages obtained by SG-OSL. For Antibes, the coherence between multigrain and single grain measurements, confirming a good bleaching degree, has already been demonstrated (Urbanová *et al.*, 2016). For Chassenon, only one out of four samples could be dated because of the insufficient quantity of quartz grains in the other three mortars. Since the factor of poor bleaching is eliminated for these series

Table 6. *Evaluation of bleaching degree: expected archaeological dose, the lowest and the highest measured equivalent dose, the ratio between the expected dose and minimum dose R_{min} and between the maximum dose and the expected dose R_{max} and the over-dispersion.*

Site	Sample	Expected dose (Gy)	Min (Gy)	Max (Gy)	R_{min}	R_{max}	R_{max}/R_{min}	OD (%)
Antibes	BDX 16045	3.70	1.14	8.46	3	2	0.7	31
	BDX 16046	3.55	1.00	10.88	4	3	0.9	31
	BDX 16047	4.70	1.18	11.84	4	3	0.6	43
	BDX 16048	4.30	1.65	9.76	3	2	1.9	27
	BDX 16049	3.85	1.69	12.74	2	3	1.5	36
Chassenon	BDX 15636	12.65	4.74	28.38	3	2	0.8	45
Palais-Gallien	BDX 15541	2.87	1.78	187.20	2	65	40	121
	BDX 15542	3.29	1.60	163.27	2	50	24	129
	BDX 15543	2.70	1.84	270.51	1	100	68	148
	BDX 15544	2.49	1.35	267.46	2	107	58	144
St Seurin	BDX 16492	1.26–1.94	1.09	79.62	1–2	32–54	14	129
	BDX 16493	1.09–1.82	1.06	91.92	1–2	51–84	29	128
	BDX 16496	4.09	3.57	179.62	1	44	38	96
	BDX 16498	4.78	2.90	188.61	2	39	24	106
	BDX 16500	1.51–2.52	1.27	108.33	1–2	43–72	22	117
	BDX 16592	0.90	0.79	147.66	1	164	144	136
	BDX 16593	0.74	0.65	151.03	1	204	179	148
	BDX 16594	0.69	0.64	140.94	1	204	189	134
	BDX 16586	0.88–1.06	1.07	194.89	1	184–221	186	157
	BDX 16587	0.81–0.97	1.05	161.81	1	167–200	181	148
Bale	BDX 16304	2.00–2.09	0.55	15.97	4	8	2	48
	BDX 16293	1.30–1.84	0.41	4.71	3–4	3	0.6	49
	BDX 16299	1.56–2.20	1.06	6.21	1–2	3	1.4	47

of samples ($\sigma_x = 0$), the over-dispersion value measured for these samples arises from the combination of microdosimetric variations and intrinsic variability ($\sigma^2 = \sigma_m^2 + \sigma_a^2$). By subtracting σ_a^2 (the square of OD DRT) from σ^2 (the square of OD ED) (**Table 4**) and subsequent root extraction, we obtain the contribution of microdosimetric variations to the dispersion of ED distributions, equal approximately to 32% for Antibes samples (average for five samples)and 45% for Chassenon. Despite this fact, the use of the central age model for the determination of the archaeological dose leads to a correct estimation of the ages.

The Basel samples present some particularities and have to be discussed separately. As mentioned before, 5 out of 8 Basel samples did not emit any OSL signal. The age of the Basel Roman sample BDX 16304 is overestimated despite its good bleaching. Based on petrographic observations, it is possible that an important quantity of luminescent quartz grains originates from crushed brick fragments present in this mortar. The annual dose rate of these grains is higher than the average annual dose rate determined by gamma spectrometry measurements, since the brick fragments are more radioactive than the rest of the mortar matrix (**Fig. 4**). Such discrepancy can explain the final over-estimation of the age of the sample BDX 16304. This example demonstrates the importance of the preliminary characterization of mortar for the correct interpretation of the results.

The samples BDX 16293 and BDX 16299 were very weakly luminescent (less than 0.5% of grains gave the signal). For reasons of time constraints, these samples were analyzed by multigrain technique and a complementary SG-OSL analysis was performed only for the sample BDX 16299. Even if we considered the probability of the presence of more than one luminescent grain per disc as relatively low, the SG-OSL measurement showed the presence of some poorly bleached grains on 2 out of 6 single grain discs (**Table 8**). This observation explains the over-estimation of the age obtained for the sample BDX 16299. It may be therefore concluded that even for such weakly luminescent samples, an averaging effect occurs when using the multigrain technique (Jain *et al.*, 2004) and its use should be avoided as much as possible if we want to obtain reliable dating results.

Poorly bleached mortars

Due to a large scatter of ED values, the archaeological dose in the case of poorly bleached samples was calculated by using the following models:

- 3-parameter minimum age model (MAM-3, Galbraith *et al.*, 1999)
- 4-parameter minimum age model (MAM-4, Galbraith *et al.*, 1999)
- internal-external consistency criterion (IEU, Thomsen *et al.*, 2003 and 2007)

To run these models, an input parameter σ_b (corresponding to a for IEU) defining the expected scatter of

Table 7. *Recapitulative table of dating results for samples emitting SG-OSL signal.*

Sample	Reference date (years)	Water content[I] (%)	Annual dose (mGy/year)	Archeo dose[II] (Gy)	Nb of grains[III]	σ/a[IV] (%)	Date (years)
Grimaldi castle, Antibes							
BDX 16045		5.0 ± 2.5	1.83 ± 0.07	3.85 ± 0.10 (CAM)	196	31	–86 ± 100
BDX 16046		6.0 ± 3.0	1.72 ± 0.08	3.56 ± 0.09 (CAM)	180	31	–62 ± 104
BDX 16047	31 ± 40	13.0 ± 6.5	2.29 ± 0.17	4.60 ± 0.16 (CAM)	175	43	16 ± 137
BDX 16048		10.0 ± 5.0	2.07 ± 0.13	3.66 ± 0.08 (CAM)	189	27	216 ± 110
BDX 16049		13.0 ± 6.5	1.92 ± 0.14	3.89 ± 0.13 (CAM)	152	36	183 ± 156
Thermal baths of Chassenon							
BDX 15636	130 ± 48	10.0 ± 5.0	6.76 ± 0.38	12.73 ± 0.77 (CAM)	61	45	131 ± 131
***Palais-Gallien*, Bordeaux**							
BDX 15541		10.0 ± 5.0	1.51 ± 0.07	3.07 ± 0.12 (IEU)	37	15	–18 ± 90
BDX 15542	109 ± 41	8.0 ± 4.0	1.73 ± 0.09	3.39 ± 0.21 (IEU)	26	25	55 ± 128
BDX 15543		8.0 ± 4.0	1.42 ± 0.05	2.91 ± 0.12 (IEU)	28	15	–41 ± 94
BDX 15544		12.0 ± 6.0	1.31 ± 0.07	2.51 ± 0.10 (IEU)	25	15	99 ± 86
Saint Seurin crypt, Bordeaux							
BDX 16492	>450, <1000	7.0 ± 3.5	1.24 ± 0.03	1.73 ± 0.04 (IEU)	71	14	574 ± 68
BDX 16493	>450, <1000	7.0 ± 3.5	1.21 ± 0.05	1.81 ± 0.05 (IEU)	50	12	523 ± 71
BDX 16496	433 ± 129	3.0 ± 1.5	2.56 ± 0.09	-	-	-	-
BDX 16498	433 ± 129	3.0 ± 1.5	2.99 ± 0.09	-	-	-	-
BDX 16500	433 ± 129	8.0 ± 4.0	1.68 ± 0.08	2.74 ± 0.13 (IEU)	56	30	386 ± 107
Saint Seurin, apse, Bordeaux							
BDX 16592		5.0 ± 2.5	1.29 ± 0.06	1.09 ± 0.06 (IEU)	15	10	1170 ± 58
BDX 16593	1150 ± 50	5.0 ± 2.5	1.00 ± 0.05	1.13 ± 0.06 (IEU)	16	10	945 ± 74
BDX 16594		5.0 ± 2.5	0.98 ± 0.04	1.00 ± 0.06 (IEU)	15	10	999 ± 71
Saint Seurin, chapel, Bordeaux							
BDX 16586	1444	5.0 ± 2.5	1.76 ± 0.10	1.29 ± 0.09 (IEU)	5	7	1301 ± 59
BDX 16587	1444	5.0 ± 2.5	1.61 ± 0.09	1.20 ± 0.10 (IEU)	4	7	1271 ± 68
Basel cathedral (crypt)							
BDX 16304	310 ± 40	13.0 ± 6.5	1.20 ± 0.06	2.86 ± 0.15 (CAM)	100	49	–368 ± 168
BDX 16293*	550 ± 250	-	1.07 ± 0.06	1.60 ± 0.15 (CAM)	29 discs	47	520 ± 160
BDX 16299*	550 ± 250	-	1.28 ± 0.07	2.51 ± 0.21 (CAM)	34 discs	48	55 ± 196

[I] water content used for age determination
[II] archaeological dose calculated using either Central age model (CAM) or internal external consistency criterion (IEU)
[III] number of grains taken into account for age calculation
[IV] over-dispersion value σ calculated from CAM/input parameter a used to run the IEU model
** samples BDX 16293 and BDX 16299 were analyzed by multigrain technique*

Table 8. *Single grain measurements of the sample BDX 16299 (Basel mortar).*

Disc	Grain (order)	ED (Gy)
1	64	2.08 ± 0.36
1	91	29.03 ± 5.38
3	51	2.10 ± 0.45
6	5	43.58 ± 8.06
7	34	10.67 ± 3.47
8	25	3.30 ± 0.70
9	65	3.03 ± 0.54
12	27	8.92 ± 2.83
12	80	2.80 ± 0.73

equivalent doses in the well-bleached part of the population is needed. Due to a small quantity of material available for analyses, additional dose recovery tests on bleached but non-irradiated samples could not be performed and the b parameter in IEU model was therefore considered 0. This implies that no over-dispersion for a given dose of 0 Gy is supposed, which may slightly differ from real behavior of the samples. Given that the expected values of archaeological doses are not lower than 1 Gy, such discrepancies should not have significant effect on the age determination. The results are summed up in **Table 7**. The poorly bleached mortars analyzed in this study can be basically divided into two groups.

Small-grained mortars with low potassium content (BDX 16492-3,BDX 16592-4,BDX 16586-7)

Based on the discussion in Section 4 (Sources of dispersion in equivalent dose distributions – Microdosimetric variations in mortar samples and implications for dating), some of the mortars identified as poorly bleached were assumed to be only slightly affected by microdosimetric variations, principally due to the low potassium content and small-grained character. Then, since the factor of microdosimetric variations is eliminated ($\sigma_m = 0$)

for these series of samples, the over-dispersion value measured arises from the combination of poor bleaching and intrinsic variability ($\sigma^2 = \sigma_x^2 + \sigma_a^2$). Supposing the transmissibility of DRT to the ED measurements, over-dispersion from dose recovery tests (OD DRT) will approximately correspond to the expected variability in the well bleached part of ED distribution (**Table 4**). Therefore, the value of OD DRT was taken into account as an input parameter σ_b (a) to run the above mentioned minimum models. MAM-3 and MAM-4 tended to overestimate the expected archaeological dose for the given values of OD DRT and were systematically higher than the values obtained by IEU. The dates obtained by using the IEU model are in agreement with the reference dates within one standard deviation for the samples BDX 16492-3 and BDX 16592 and within two standard deviations for the samples BDX 16593-4 (**Table 7**). The dates for the samples BDX 16586-7, which are slightly overestimated, cannot be considered as reliable since only 4–5 grains were considered to be well bleached and taken into account for final dose and age estimation.

Coarse-grained mortars with low potassium content (BDX 16496, 16498, 16500, 15541-4)

This group of poorly bleached samples was assumed (Section 4 (Sources of dispersion in equivalent dose distributions – Microdosimetric variations in mortar samples and implications for dating)) to be affected by microdosimetric variations. Therefore, the effects of poor bleaching and heterogeneous microdosimetry are overlapping ($\sigma^2 = \sigma_x^2 + \sigma_m^2 + \sigma_a^2$). We have seen (for the well bleached samples) that the contribution of microdosimetric variations to the scatter in ED distributions can be relatively significant. Without the possibility of quantifying these effects, it is very difficult to estimate the input parameter σ_b (a) which would describe correctly the scatter of equivalent doses in the well-bleached part of the population. Two hypotheses can be drawn:

1) The expected over-dispersion will not be lower than the over-dispersion from dose recovery experiments.
2) The expected over-dispersion will not be higher than 50% which is the maximum over-dispersion value obtained in our case for natural well-bleached mortars.

For each model we tried to examine how the values of archaeological dose change when the input parameter σ_b (a) is being varied between 5 and 50% (**Fig. 7**, Medialdea *et al.*, 2014). The difference between the archaeological doses obtained for the minimum and the maximum value of σ_b (a) is about 50–80% of the expected archaeological dose.

Dating results for poorly bleached samples presented in **Table 7** were obtained by the IEU model. Except for the sample BDX 15542 for which many fewer grains were analyzed, expected values of archaeological doses for *Palais-Gallien* are obtained by IEU with a about 15%, whereas for example for the sample BDX 16500 from the Saint Seurin crypt the result is with a about 30%. This is an interesting observation and the question we can ask is: what is the difference between these mortars?

A principle distinction is that the samples from Saint Seurin crypt contain coarse crushed brick fragments which are usually rich in uranium. This fact might imply important microdosimetric variations arising from the concentration of uranium besides those arising from potassium. In contrast, the content of uranium in *Palais-Gallien* mortars is quite low and the microdosimetric variations are assumed to arise mainly from potassium feldspars (Urbanová *et al.*, 2015).

The a value of 15% taken into account to obtain the expected archaeological dose for samples BDX 15541 and BDX 15543 is equal to the over-dispersion from dose recovery tests. According to our hypothesis, higher value of over-dispersion in the well-bleached part of the population affected in this case by microdosimetric variations would be expected. One possible explanation is that since dose recovery tests of the samples from *Palais-Gallien* were performed on the grains bleached in the solar simulator, it might have caused an undesirable increase in the signal as discussed in Section 4 (Sources of dispersion in

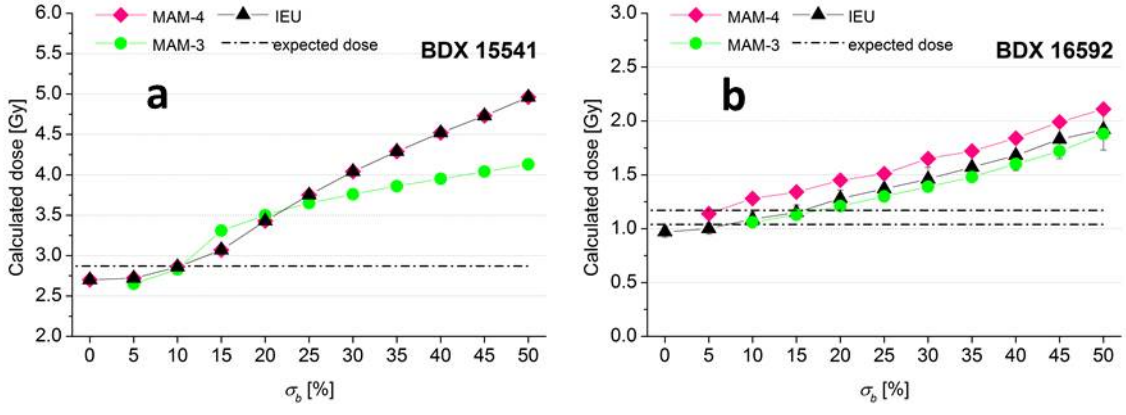

Fig. 7. *Dependence of the archaeological dose (paleodose) calculated according to minimum age models on the input parameter* σ_b *(a).*

equivalent dose distributions – Intrinsic variability). Unfortunately, the comparison with the bleaching in the OSL reader was not possible in this particular case due to the lack of material.

For the samples BDX 16496 and BDX 16498 from the Saint Seurin crypt, we do not present any dating results. Even a visual evaluation of extremely scattered ED distributions without any particular frequency peak indicates that the use of the IEU model, focusing on the lowest normal population, is not suitable in this case.

In some cases, the use of the MAM-3 and the IEU model resulted in similar values of archaeological dose. However, in some cases, the results of MAM-3 and MAM-4 were not consistent. For the low values of $\sigma_b\,(a)$, the archaeological doses obtained by using the MAM-4 (and MAM-3 in some cases) were higher than those from the IEU and tended to over-estimate the expected archaeological dose. The slight tendency of MAM-3 and MAM-4 for over-estimation was already stated for young and less sensitive samples (Sim *et al.*, 2013; Medialdea *et al.*, 2014). Moreover, in many cases the experimental data could not be fitted when using MAM-3 and MAM-4 which resulted mainly in it being impossible to obtain the *p* parameter. In these cases, the archaeological dose could not be calculated when using these models.

When applying the IEU, the results were generally in good agreement with expected archaeological doses if there was a significant frequency peak in the lowest dose region. Similar conclusions have been already drawn for other series of young samples (Sim *et al.*, 2013; Medialdea *et al.*, 2014). However, in both cases, either when using MAM or IEU, the calculated archaeological dose is dependent on the input parameter $\sigma_b\,(a)$. To estimate this parameter, which is a priori unknown, we suggest taking into account the over-dispersion value from dose recovery experiments and hypotheses on microdosimetric variations deduced from beta autoradiography and variations of K content.

To conclude, for poorly bleached, coarse grained mortars, we attempted to explain the difficulties encountered when trying to calculate the archeological dose. However, no satisfactory and universal procedure of the right archaeological dose determination that could be suggested in order to estimate the age of non-dated samples was found. Nevertheless, many important aspects that complicate the dating procedure of such problematic samples have been identified and are currently being investigated and are discussed in following paragraphs.

CONCLUSION

In this paper, a three year study on dating archaeological mortars by SG-OSL has been reviewed, attempting to show and compare samples from different geological areas. Different aspects of sampling, preparation and measurement procedures have been discussed and the principal conclusions can be presented:

- From the practical point of view, we concluded that sampling by the means of a hammer and a chisel is preferred to other techniques if possible. About 100 g of bulk samples was generally sufficient for dating purposes.
- Chemical treatment with the mixture of H_2SiF_6 with HNO_3 in a ratio of 9:1 proved to be effective in dissolving feldspars. No significant deviation was identified between equivalent doses measured after this treatment compared with treatment by HF.
- SG-OSL measurements showed systematic predominance of the fast component in an OSL signal for well-bleached quartz grains. Between 1–8% out of 4000 quartz grains analyzed per sample emitted an OSL signal.
- Due to a wide scattering in equivalent doses, the dose-response curve needs to be significantly extended to determine higher equivalent doses.
- Even if we did not observe any increase in equivalent dose with rising preheat temperature, we recommend using a preheat of 190°C as an initial parameter in order to minimize the potential risks of thermal transfer that would significantly change kinetics of luminescence. If the dose recovery tests are satisfactory, these temperatures can be kept for equivalent dose determination.
- The LM-OSL test was not always representative of the behavior of individual grains due to the averaging effects occurring when using multigrain technique.
- Well bleached mortars reached over-dispersion values of up to 50%, but not higher.

If we sum up the results for the corpus of 33 mortar samples studied in this work, four categories of samples were identified:

1) the samples for which no signal was detected by SG-OSL and therefore they could not be dated
2) the well-bleached samples that can be reliably dated by using the Central age model for the calculation of archaeological dose
3) the poorly bleached samples that are not significantly affected by microdosimetric variations and which can be dated by using intrinsic variability as an input parameter to run an IEU model
4) the poorly bleached samples highly affected by poor bleaching and heterogeneous microdosimetry for which the universal method of archaeological dose evaluation has not been found yet

The results indicate that small-grained mortar and mortar that contains low amounts of potassium feldspars will probably be easier to date. The mortars that contain crushed brick fragments (so-called *cocciopesto* mortars in the literature) are generally more problematic for dating due to the differences between the radioactivity of the bricks and the mortar matrix itself.

The crucial conclusion that we can draw on the basis of the results obtained is that problematic mortar samples from the fourth category can be identified by combining

single grain OSL analyses with material characterization. Therefore, the validity of the dating result can be easily evaluated. In conclusion, we underline the importance of material characterization which should make an inseparable part of the dating process.

In this study, suitability of the single grain technique when dating the incompletely bleached mortars has been shown. Even if in some studies small aliquots have also been proven useful for dating of poorly bleached young samples, we would still recommend analyzing at least a small number of single grain discs for dim samples as preliminary step in order to check the character of the material studied (the proportion of luminescent grains and the ratio of the well bleached grains to the poorly bleached ones). In the case of mortars, usually a very small quantity of the sample is available for dating. In addition, these samples generally contain very low percentage of luminescent grains (1–7%) and often even lower proportion of the well bleached grains. The use of small aliquots can therefore be a bit "risky" since much more material can be consumed when "losing" a part of the well bleached grains, being hidden at the same disc with the poorly bleached ones (as shown for the sample BDX 16299 in our experiment, **Table 8** or concluded also for example by Jain *et al.*, 2004 or Arnold *et al.*, 2012). For well bleached mortars from Antibes, the single grain and the multigrain measurements provided both satisfactory results.

Difficulties encountered and potential solutions

Need of more suitable age models

The principal difficulty of existing minimum age models is that an input parameter is needed to run the model, and the right estimation of this parameter is very complicated for mortars affected by both poor bleaching and heterogeneous microdosimetry. The MAM-3 and MAM-4 often fail to fit experimental parameters. The IEU gave quite satisfactory results in many cases, however, it seems to work mainly if there is a significant frequency peak in the lowest dose region of ED distributions since the model aims at the lowest Gaussian distribution (provided that the input parameter correctly describes the data). Nevertheless, the model is not adapted for the evaluation of the distributions of extremely poorly bleached mortars when the form of the beginning of the distribution deviates from the Gaussian one. Alternative models that seem to be better adapted for the series of samples studied are being developed and tested on the data acquired in this work (Guibert *et al.*, submitted; Christophe *et al.*, submitted).

Imprecision in quantification of microdosimetric variations

Currently, it is not possible to quantify with satisfactory precision the microdosimetric variations to which natural archaeological samples are subjected. Beta autoradiography enables the study of the distribution of beta emissions in the matrix, however, it does not make it possible to distinguish between different emitting radioelements (Ruffer and Preusser, 2009). EDX-SEM cartography allows indirect mapping of the distribution of potassium, but not of uranium and thorium. Such mapping of all three radioelements can be performed by ICP-MS analyses, if available. In addition, the distribution of uranium and thorium could potentially be studied via the distribution of alpha irradiations by using SSNTD detectors (Sanzelle *et al.*, 1986; Wagner *et al.*, 2005; Grainger, 2009). A priori, low background gamma spectrometry measurements of K, U and Th allow the identification of the predominant beta emitting radioelement.

Currently, different approaches aimed at a quantification of microdosimetric variations in archaeological materials by means of computer simulations (Martin *et al.*, 2015; Lebrun *et al.*, in preparation) are being developed. The integration of these approaches for the samples presented in this study might be attempted in future.

Perspectives

The study shows the indisputable potential of SG-OSL in dating archaeological mortars, material whose bleaching results from complex anthropic activity initially employing much older geological sediments. To reinforce the methodology and to confirm the conclusions of this study, a larger number of mortar samples needs to be studied. Also, single grain dating of smaller fractions (90–125 μm) will be tested for the comparison with the coarse ones. The method is actually being applied on five other monuments, each of them containing chronological sequences from Antiquity to the High Middle Ages period. The SG-OSL measurements show the series of well-bleached mortar samples at least for one of these sites (Renaissance chapel in Périgueux, France), where SG-OSL dating helps to pinpoint the chronology of different construction phases of the building. As mentioned above, in the case of poorly bleached samples new approaches to determine the archeological dose are being tested.

ACKNOWLEDGMENTS

We are grateful to the following organizations which have supported this research financially: CNRS-INSHS [French National Center for Scientific Research - Institute of Human and Social Sciences], Conseil Régional d'Aquitaine [equipment], University Bordeaux-Montaigne [PhD grant and special support for research programs], Mairie d'Antibes, Conseil Régional de la Charente, Mairie de Bordeaux. This project was co-financed by the labex LaScArBx [Bordeaux Archaeological Sciences Labex] administrated by ANR [Agence Nationale de la Recherche] with the reference ANR-10-LABX-52. We would also like to express our thanks to the following institutions for the authorization to sample the studied monu-

ments: Mairie de Bordeaux, Service Régional de l'Archéologie d'Aquitaine, Service des Monuments Historiques, Conseil Général de la Charente, Mairie d'Antibes, Musée Picasso and Service cantonale d'archéologie de Bâle. Special thanks to Eric Delaval, to David Hourcade, to Anne Michel, Martin Allemann, Marco Bernasconi, Sophie Hueglin, Claude Ney, Yannick Lefrais, Brigitte Spiteri, Nadia Cantin, Guillaume Guérin.

REFERENCES

Arnold LJ, Roberts R, Galbraith R and DeLong RF, 2009. A revised burial dose estimation procedure for optical dating of young and modern-age sediments. *Quaternary Geochronology* 4: 306–325, DOI 10.1016/j.quageo.2009.02.017.

Arnold LJ, Demuro M and Navazo Ruiz M, 2012. Empirical insights into multi-grain averaging effects from 'pseudo' single-grain OSL measurements. *Radiation Measurements* 47: 652–658, DOI 10.1016/j.radmeas.2012.02.005.

Blain S, Guibert P, Bouvier A, Vieillevigne E, Bechtel F, Sapin C and Baylé M, 2007. TL-dating applied to building archaeology: The case of the medieval church Notre-Dame-sous-Terre (Mont-Saint-Michel, France). *Radiation Measurements* 42: 1483–1491, DOI 10.1016/j.radmeas.2007.07.015.

Bøtter-Jensen L, Solongo S, Murray AS, Banerjee D and Jungner H, 2000. Using OSL single-aliquot regenerative-dose protocol with quartz extracted from building materials in retrospective dosimetry. *Radiation Measurements* 32(5–6): 841–845, DOI 10.1016/S1350-4487(99)00278-4.

Brennan BJ, Lyons RG and Phillips SW, 1991. Attenuation of alpha particle track dose for spherical grains. *International Journal of Radiation Applications and Instrumentation. Part D. Nuclear Tracks and Radiation Measurements* 18: 249–253, DOI 10.1016/1359-0189(91)90119-3.

Bulur E, Duller GAT, Solongo S, Bøtter-Jensen L and Murray A, 2001. LM-OSL from single grains of quartz: a preliminary study. *Radiation Measurements* 35: 79–85, DOI 10.1016/S1350-4487(01)00256-6.

Christophe C, Philippe A, Guérin G, Mercier N and Guibert P, submitted. A Bayesian model for the OSL dating of poorly bleached sediment samples. *Radiation measurements*.

Choi JH, Murray AS, Cheong CS and Hong SC, 2009. The dependence of dose recovery experiments on the bleaching of natural quartz OSL using different light sources. *Radiation Measurements* 44: 600–605, DOI 10.1016/j.radmeas.2009.02.018.

Fisher A, 2008. Archäologie in Basel. (Archaeology in Basel). Unter uns, 255, Basel, p. 255. (in French).

Galbraith RF, Roberts RG, Laslett GM, Yoshida H and Olley JM, 1999. Optical dating of single and multiple grains of quartz from Jinmium Rock Shelter, Northern Australia: part I, experimental design and statistical models. *Archaeometry* 41(2): 339–364, DOI 10.1111/j.1475-4754.1999.tb00987.x.

Grainger S, 2009. *Development of techniques for high-resolution spatially resolved elemental analysis in materials of interest in luminescence dating.* Master thesis, Durham university, Great Britain.

Goedicke C, 2011. Dating mortar by optically stimulated luminescence: a feasibility study. *Geochronometria* 38(1): 42–49, DOI 10.2478/s13386-011-0002-0.

Goedicke C, 2003. Dating historical calcite mortar by blue OSL: results from known age samples. *Radiation Measurements* 37: 409–415, DOI 10.1016/S1350-4487(03)00010-6.

Gueli AM, Stella G, Troja SO, Burrafato G, Fontana D, Ristuccia GM and Zuccarello AR, 2010. Historical buildings: Luminescence dating of fine grains from bricks and mortar. *Il Nuovo cimento* 125B, DOI 10.1393/ncb/i2010-10892-4.

Götze J, Plötze M and Habermann D, 2001. Origin, spectral characteristics and practical applications of the cathodoluminescnece (CL) of quartz - a review. *Mineralogy & Petrology* 71: 225–250, DOI 10.1007/s007100170040.

Guérin G, Combès B, Lahaye C, Thomsen K, Tribolo C, Urbanova P, Guibert P, Mercier N and Valladas H, 2015. Testing the accuracy of a Bayesian central-dose model for single-grain OSL, using known-age samples. *Radiation Measurements* 74: 1–9, DOI 10.1016/j.radmeas.2015.04.002.

Guérin G, Myank J, Thomsen K, Murray A and Mercier N, 2015. Modelling dose rate to single grains of quartz in well-sorted sand samples: The dispersion arising from the presence of potassium feldspars and implications for single grain OSL dating. *Quaternary Geochronology* 27: 52–65, DOI 10.1016/j.quageo.2014.12.006.

Guérin G, Mercier N and Adamiec G, 2011. Dose-rate conversion factors: update. *Ancient TL* 29: 5–8.

Guibert P, Christophe C, Urbanova P, Guérin G and Blain S, 2000. Modeling incomplete and heterogeneous bleaching of mobile grains partially exposed to the light: towards a new tool for single grain OSL dating of poorly bleached mortars. *Radiation Measurements*. Submitted.

Guibert P, Bailiff IK, Blain S, Gueli AM, Martini M, Sibilia E, Stella G and Troja S, 2009a. Luminescence dating of architectural ceramics from an early medieval abbey: the St-Philbert intercomparison (Loire Atlantique, France). *Radiation Measurements* 44: 488–493, DOI 10.1016/j.radmeas.2009.06.006.

Guibert P, Lahaye C and Bechtel F, 2009b. The importance of U-series disequilibrium of sediments in luminescence dating: a case study at the Roc de Marsal cave (Dordogne, France). *Radiation Measurements* 44: 223–231, DOI 10.1016/j.radmeas.2009.03.024.

Guibert P and Schvoerer M, 1991. TL-dating: Low background gamma spectrometry as a tool for the determination of the annual dose. *Nuclear Tracks Radiation Measurements* 18(1–2): 231–238, DOI 10.1016/1359-0189(91)90117-Z.

Hourcade D and Maurin L, 2013. Mars Grannus à Cassinomagus (Chassenon, Charente). *Aquitania* 29: 137–153. (in French).

Hourcade D, Calamy L, Méaudre JC, Morin T, Robert B and Soulas S, 2010.*Thermes de Longeas: Le rez de chaussée des thermes. Cour de chauffe et systèmes de soutènement des thermes de Chassenon. Report 2012, (Longeas thermal baths: ground floor of the baths. Heating yard and supporting system of thermal baths in Chassenon. Report 2012)*, SRA Pointou-Charentes, SRA Pointou-Charentes.

Hourcade D, 2013. Amphithéâtre du Palais-Gallien (Palais-Gallien amphitheatre). 80–88 In: C. Doulan (dir.), *Bordeaux Carte archéologique de la Gaule* 33(2): Paris.

Hourcade D, Bernard K, Bost JP, Coutelas A, Doulan C, Espinasse L, Guibert P, Jean-Courret E, Maleret S, Meunier C, Michel C, Mora P, Morin T, Piot A, Régaldo P, Sanchez C, Sireix C and Soulas S, 2011. Le Palais-Gallien de Bordeaux. Histoire et architecture (2010–2012). (Palais-Gallien of Bordeaux. History and architecture (2010–2012)). *Rapport 2011*, 3 vol., SRA Aquitaine, 900 p. (in French).

Hueglin S, 2011. Medieval Mortar Mixers Revisited. Basle and Beyond. *Zeitschrift für Archäologie des Mittelalters* 39: 189–212.

Jacobs Z, Duller GAT, Wintle AG, 2006. Interpretation of single grain De distributions and calculation of De. *Radiation Measurements* 41: 264-277, DOI 10.1016/j.radmeas.2005.07.027.

Jacobs Z, Hayes EE, Roberts GR, Galbraith RF and Henshilwood CS, 2013. An improved OSL chronology for the Still Bay layers at Blombos Cave, South Africa: further tests of single-grain dating procedures and a re-evaluation of the timing of the Still Bay industry across southern Africa. *Journal of archaeological science* 40: 579–594, DOI 10.1016/j.jas.2012.06.037.

Jain M, Thomsen KJ, Bøtter-Jensen L and Murray AS, 2004. Thermal transfer and apparent-dose distributions in poorly bleached mortar samples: results from single grains and small aliquots of quartz. *Radiation Measurements* 38: 101–109, DOI 10.1016/j.radmeas.2003.07.002.

Krbetschek MR, Göetze J, Dietrich A and Trautmann T, 1998. Spectral information from minerals relevant for luminescence dating. *Radiation Measurements* 27: 695–748, DOI 10.1016/S1350-4487(97)00223-0.

Lanos P and Dufresne P, 2013. Chassenon (Charente) Thermes de Cassinmagus, Cave 10. Analyse archéomagnétique. (Chassenon (Charente) Cassinmagus thermal baths, Cave 10. Archeomagnetic analyses). *Rapport 2013.* (in French).

Lanos P and Dufresne P, 2013. Antibes (Alpes-Maritimes), Château Grimaldi, Mur MR 10003. Analyse archéomagnétique. (Antibes (Alpes-Maritimes), Grimaldi Castle, Wall MR 10003. Archeomagnetic analyses). *Rapport 2013.* (in French).

Lanos P and Dufresne P, 2013. Palais-Gallien (Bordeaux). Analyse archéomagnétique. (Palais-Gallien (Bordeaux). Archeomagnetic analyses). *Rapport 2013.* (in French).

Lebrun B, Tribolo C, Martin L and Mercier N, in preparation. Assessing OSL equivalent doses dispersion through sediment modeling: a case study of dose rate heterogeneities simulation for West African sediments. (*UK Luminescence and ESR Meeting 2016* Liverpool) in preparation.

Liritzis I, Mavrikis D, Zacharias N, Sakalis A, Tsirliganis N and Polymeris GS, 2011. Potassium determinations using SEM, FAAS and XRF: Some experimental notes. *Mediterranean Archaeology and Archaeometry* 11(2): 169–179.

Martin L, Mercier N, Incerti S, Lefrais Y, Pecheyran C, Guérin G, Jarry M, Bruxelles L, Bon F and Pallier C, 2015. Dosimetric study of sediments at the beta dose rate scale: Characterization and modelization with the DosiVox software. *Radiation Measurements* 81: 134–141, 10.1016/j.radmeas.2015. 02.008.

Mayya YS, Mortheka P, Murari MK and Singhvi AK, 2006. Towards quantifying beta microdosimetric effects in single-grain quartz dose distribution. *Radiation Measurement*s 41: 1032–1039, DOI 10.1016/j.radmeas.2006.08.004.

Medialdea A, Thomsen KJ, Murray AS and Benito G, 2014. Reliability of equivalent-dose determination and age-models in the OSL dating of historical and modern palaeoflood sediments. *Radiation Measurements* 22: 11–24, DOI 10.1016/j.quageo.2014.01.004.

Mejdahl V, 1979. Thermoluminescence dating: beta-dose attenuation in quartz grains. *Archaeometry* 21: 61–72, DOI 10.1111/j.1475-4754.1979.tb00241.x.

Michel A, 2012. Autour de l'identification des mausolées: le cas de Saint-Seurin de Bordeaux. Mausolées & Églises, IV^{e}-VIII^{e} siècle. (About the identification of mausoleums: case study of Saint Seurin in Bordeaux. Mausolées & Churches, IVth-VIIIth century, Hortus Artium Medievalium). *Hortus Artium Medievalium*, 18(2). (in French).

Murray AS and Roberts RG, 1998. Measurement of the equivalent dose in quartz using a regenerative-dose single-aliquot protocol. *Radiation Measurements* 29: 503–515, DOI 10.1016/S1350-4487(98)00044-4.

Murray AS and Wintle A, 2000. Luminescence dating of quartz using an improved single-aliquot regenerative dose protocol. *Radiation Measurements* 32: 523–538, DOI 10.1016/S1350-4487(99)00253-X.

Murray AS and Olley JM, 2002. Precision and accuracy in the optically stimulated luminescence dating of sedimentary quartz: a status review. *Geochronometria* 21: 1–16.

Panzeri L, 2013. Mortar and surface dating with optically stimulated luminescence (OSL): innovative techniques for the age determination of buildings. *Nuovo Cimento della* 36(4): 205–216.

Pietzch TJ, Olley JM and Nanson GC, 2008. Fluvial transport as a natural luminescence sensitiser of quartz. *Quaternary Geochronology* 3: 365–376, DOI 10.1016/j.quageo.2007.12.005.

Ruffer D and Preusser F, 2009. Potential of autoradiography to detect spatially resolved radiation patterns in the context of trapped charge dating. *Geochronometria* 34: 1–13, DOI 10.2478/v10003-009-0014-4.

Sanzelle S, Fain J and Mailler D, 1986. Theoretical and experimental study of alpha counting efficiency using LR-115 Kodak SSTND applied to dosimetry in the field of thermoluminescence dating. *International Journal of Radiation Applications and Instrumentation.* Part D. *Nuclear Tracks and Radiation Measurements* 12: 913–916, DOI 10.1016/1359-0189(86)90733-8.

Sim AK, Thomsen KJ, Murray AS, Jacobsen G, Drysdale R and Erskine W, 2013. Dating recent floodplain sediments in the Hawkesbury-Nepean river system using single grain quartz OSL. *Boreas* 43(1): 1–21, DOI 10.1111/bor.12018.

Stella G, Fontana D, Gueli AM and Troja SO, 2013. Historical mortars dating from OSL signals of fine grain fraction enriched in quartz. *Geochronometria* 40(3): 153–164, DOI 10.2478/s13386-013-0107-8.

Thomsen KJ, Murray A and Jain M, 2012. The dose dependency of the over-dispersion of quartz OSL single grain dose distributions. *Radiation Measurements* 47: 732–739, DOI 10.1016/j.radmeas.2012.02.015.

Thomsen KJ, Murray AS, Bøtter-Jensen L and Kinahan J, 2007. Determination of burial dose in incompletely bleached fluvial samples using single grains of quartz. *Radiation Measurements* 42(3): 370–379, DOI 10.1016/j.radmeas.2007.01.041.

Thomsen KJ, Murray A and Bøtter-Jensen L, 2005. Sources of variability in OSL dose measurements using single grains of quartz. *Radiation Measurements* 39: 47–61, DOI 10.1016/j.radmeas.2004.01.039.

Thomsen KJ, Jain M, Bøtter-Jensen L, Murray AS and Jungner H, 2003. Variation with depth of dose distributions in single grains of quartz extracted from an irradiated concrete block. *Radiation Measurements* 37: 315–321, DOI 10.1016/S1350-4487(03)00006-4.

Urbanová P, Hourcade D, Ney C and Guibert P, 2015. Sources of uncertainties in OSL dating of archaeological mortars: the case study of the Roman amphitheatre *Palais-Gallien* in Bordeaux. *Radiation Measurements* 72: 100–110, DOI 10.1016/j.radmeas.2014.11.014.

Urbanová P, Delaval E, Dufresne P, Lanos P and Guibert P, 2016. Multi-method dating comparison of Grimaldi castle foundations in Antibes, France. *ArchéoSciences - Revue d'archéométrie*, 40: 17–33.

Urbanová P and Guibert P, 2017. La mesure du temps par luminescence: datation de réemplois dans la crypte de Saint Seurin à Bordeaux. Dossier « Atelier doctoral. Les remplois en architecture entre Antiquité et Moyen Âge » of *Mélanges de l'École française de Rome*. (Measurement of time by luminescence: dating of spolia in the crypt of Saint Seurin, Bordeaux. Dossier « Doctoral atelier. Reuse in architecture between Antiquity and Middle Ages » of Mélanges de l'École française de Rome). 129, 1. (in French).

Wagner GA, Glasmacher UA and Greilich S, 2005. Spatially resolved dose-rate determination in rocks and ceramics by neutron-induced fission tracks: fundamentals. *Radiation Measurements* 40: 26–31, DOI 10.1016/j.radmeas.2004.09.005.

Wintle AG and Murray AS, 2006. A review of quartz optically stimulated luminescence characteristics and their relevance in single-aliquot regeneration dating protocols. *Radiation Measurements* 41(4): 369–391, DOI 10.1016/j.radmeas.2005.11.001.

Zacharias N, Mauz B and Michael CT, 2002. Luminescence quartz dating of lime mortars. A first research approach. *Radiation Protection Dosimetry* 101: 379–382.